NASA Contractor Report 172361

APPLICATION OF SELECTED ADVANCED TECHNOLOGIES
TO HIGH PERFORMANCE, SINGLE-ENGINE,
BUSINESS AIRPLANES

NASA-CR-172361
19840019651

Christopher S. Domack and Glenn L. Martin

Kentron International, Inc.
Aerospace Technologies Division
Hampton, Virginia 23666

NASA

National Aeronautics and
Space Administration

Langley Research Center
Hampton, Virginia 23665

SUMMARY

A study was conducted to determine the effects of selected technology improvements on the fuel efficiency and performance of a six-place, single-engine propeller driven business airplane. The technologies examined included natural laminar flow, an advanced diesel engine, composite material airframe construction, and pusher versus tractor configuration design. Five airplane configurations were developed, each of which can carry six people with baggage for a no wind, no reserve range of 1,300 n.mi. at cruise speeds of over 275 kt at altitudes of 30000 ft and above. The baseline airplane for comparison purposes was a conventionally configured, all aluminum, six-place, single-engine turboprop developed previously.

The study results showed that, of the technologies examined, natural laminar flow produced the most significant performance gains, while the advanced diesel engine provided greatly enhanced fuel efficiency at a moderate expense in performance. Due to other tradeoffs, the net gains from composite construction and pusher configuration design were not as significant as expected. The study also indicated the need for a more comprehensive database of airfoil sections designed for natural laminar flow characteristics in order to promote further application of this technology.

INTRODUCTION

The general aviation airplane is a mainstay of American business transportation. A sizable number of these airplanes are six to eight passenger twin-engine turboprops or turbofans capable of servicing relatively short or unimproved landing sites. They provide the business community with transportation comfort and flexibility unmatched by scheduled air carrier service.

Current economic conditions have magnified the importance of the general aviation business airplane, particularly since deregulation of the commercial airlines has led to significant changes in the scheduled air service to many cities. Corporate aircraft are increasingly perceived as a necessity by many businesses; however, most current business aircraft are relatively expensive to procure, operate, and maintain. This leads to deferral or elimination of an

1

N84-27719

aircraft purchase, a situation clearly evidenced by the large drop in industry sales in recent years.

The drop in general aviation airplane sales may be partially attributed to the reluctance of the manufacturers to incorporate advanced technologies into these aircraft, a consequence of the high costs of existing production tooling, airplane certification, and potential product liability judgments. Despite these obstacles, there is clearly a need for continued development of less costly, more efficient business airplanes. The long-term survival of the industry may well depend on the incorporation of the advanced aerodynamic, propulsion, and structural technologies now evolving.

The National Aeronautics and Space Administration (NASA) and the aerospace industry are involved in continuing efforts to improve the efficiency and safety of this class of aircraft. A previous NASA-sponsored study (ref. 1) has shown that a single-engine turboprop business airplane could be configured with present technology to provide substantially better fuel efficiency than conventional twin-engine turboprops with comparable speed, range, payload, and comfort. The airplane of reference 1 (designated GATP-1A, see fig. 1) accomplished these goals using existing and entirely conventional general aviation technology. Performance requirements included a maximum cruise speed of at least 300 kt at or above 30,000 ft, carrying six people with baggage for a no wind, no reserve range of 1,300 n. mi.

The current study sought to investigate the potential for even greater fuel efficiency and performance through the use of selected technology improvements which were not incorporated into the GATP-1A configuration. These improvements included natural laminar flow (NLF), an advanced diesel engine, composite material airframe construction, and pusher configuration layout. All the advanced technologies analyzed, except for the advanced diesel engine, are sufficiently developed to be considered for production aircraft. This was a key criterion for technology incorporation throughout the course of the design cycle for each study airplane. While no cost analyses were performed, it was desired to keep the level of complexity at or below traditional levels to help minimize manufacturing difficulty and cost when incorporating the advanced technologies. All study airplanes were configured for certification under existing FAR Part 23 requirements (ref. 2).

2

A complete list of the current study requirements, along with those for the former study, is presented in table I. Appendix A of this document contains tabulated drag data calculated for each of the study airplanes.

The use of trade names or names of manufacturers in this report does not constitute an official endorsement of such products or manufacturers, either expressed or implied, by Kentron International, Inc. or the National Aeronautics and Space Administration.

SYMBOLS

c	chord
$\bar{c}$	mean aerodynamic chord length (ft)
C_D	total airplane drag coefficient
C_{D_i}	induced drag coefficient
C_{D_p}	parasite drag coefficient
C_L	total airplane lift coefficient
C_p	airfoil pressure coefficient
C_P	propeller power coefficient
D	drag (lbf)
J	propeller advance ratio
L	lift (lbf)
M	Mach number
T	thrust (lbf)
V	velocity (ktas)
V_{s_o}	power-off stall speed, landing configuration (ktas)
x/c	nondimensional fraction of chord length
Λ	wing sweep angle (deg)
Δ	increment
α	angle-of-attack (deg)
δ	deflection angle (deg)
η	propeller efficiency

Abbreviations

B.L.	boundary layer
BSFC	brake specific fuel consumption (lbm/hp-hr)
CG	center-of-gravity
FAR	Federal Aviation Regulations
LE	leading edge
MAC	mean aerodynamic chord
MLG	main landing gear

4

NACA	National Advisory Committee for Aeronautics
NASA	National Aeronautics and Space Administration
NLF	natural laminar flow
SMPG	seat nautical miles per gallon
TOGW	takeoff gross weight (lbs)
TSFC	thrust specific fuel consumption (lbm/lbf-hr)
USAF	United States Air Force

Subscripts

f	flap
LE	leading edge
max	maximum
min	minimum
s	slat

CONFIGURATION DEVELOPMENT

The study configuration of reference 1, designated GATP-1A, was used as the baseline airplane for this study. The GATP-1A was an all-aluminum, conventional tractor configuration designed to demonstrate that a single-engine turboprop airplane using existing hardware and technology could provide significant fuel savings over a twin-engine turboprop with comparable performance and utility. In order to investigate advanced technology areas such as composite airframe materials, natural laminar flow, advanced engine concepts, and unconventional configurations, a matrix of study airplane configurations was developed, consisting of two basic airframes and three different engines. To evaluate configuration-dependent effects, one airframe was configured as a buried-engine pusher and the other as a conventional tractor similar to the GATP-1A. The three engines used in the study were the Pratt and Whitney PT6A-45A turboprop, the Garrett Airesearch TPE 331-11, and a Teledyne Continental conceptual diesel engine. Four of the six possible configurations were developed and designated as: PT6A-45A tractor (GATP-1B), TPE 331-11 tractor (GATP-1C), PT6A-45A pusher (GATP-2A), and a diesel pusher (GATP-2D). A separate designation, GATP-2C, was assigned to a fully-turbulent boundary layer version of the GATP-2A. All of these airplanes retained the most desirable features of the -1A baseline, but were configured with more emphasis on drag reduction and improved utility and cabin arrangement. Table II presents a comparison of the geometry of the five new study airplanes and the -1A baseline. General arrangement drawings of each aircraft are presented in figures 2, 3, 4, and 5. The following descriptions apply to each of the new study configurations.

Fuselage

Several improved features were incorporated in the new fuselage configurations. The cabins of the study airplanes retained the cross-section shape of the -1A cabin, but were lengthened in order to provide more passenger legroom and cabin baggage volume. Seating accommodations were sized for a USAF-standard 95th percentile man (ref. 3), and resulted in a cabin that is considerably larger than that of typical six-place airplanes. The entrance door was changed to a horizontally-split airstair located such that no external steps or walkways were required on the airframe. An emergency exit was provided, as on the -1A, on the opposite side of the cabin. The cabin pressurization differential was reduced

6

from 8.25 psi to 7.5 psi, which maintains a cabin altitude of 8000 ft up to an airplane altitude of 35000 ft. Pressurized baggage storage was provided on each aircraft, whereas the -1A had only unpressurized provisions. The noses and windshields of the study aircraft were recontoured for improved overnose visibility, and the number of side windows was reduced to two per side. The latter change decreased the number of cutouts necessary in the fuselage pressure vessel, thereby providing for a more efficient fuselage structure. Full IFR avionics and instrumentation were assumed, including weather radar on the pusher versions. Figures 6 and 7 present the interior arrangement of the -1B and -2A configurations, respectively.

The wing position on the fuselage for each of the study airplanes was determined by several considerations, including aerodynamics, structural practicality, mass balance, and arrangement of other airplane components and systems. The mid-wing arrangement of the -2A configuration was chosen because it is aerodynamically very "clean," and for the particular configuration studied, may have a structural advantage over other positions. Examination of the -2A interior arrangement (fig. 7) shows that the aft cabin pressure bulkhead, firewall, forward wing mount, and main landing gear mount may be combined in a single bulkhead. This ability to tie together several major components is the single greatest structural advantage that the -2A configuration has over the -1B tractor, and should allow a lighter, more efficient fuselage structure. An additional benefit of the pusher layout is that its interior noise level would be lower than that of the tractor, since the propeller is located farther from the cabin and its slipstream does not scrub the fuselage as in a tractor configuration. Integration of the diesel engine into a mid-wing configuration was not possible. The diesel engine is too large to allow retention of the mid-wing spar carry-through structure in the same position as the turboprop, therefore, the -2D has its wing in the low position. The tractor airplanes were configured with low wings, with the wing carry-through structure passing beneath the cabin floor.

Airplane center-of-gravity calculations indicated that the pusher configurations had a larger CG travel than the tractor airplanes, primarily due to the aft-mounted propeller and drive system. The length of the aft fuselage closure on the pushers also contributed to this problem. Most pusher aircraft to date (the Lear Fan being a notable exception) have relatively short, bluff afterbodies which

generate considerable drag and require unconventional tail arrangements, such as the Cessna 337 and the Rutan Vari-Eze. The closure length of the study airplane was determined primarily by aerodynamic considerations such as fuselage fineness ratio, local turning angles to maintain attached flow, and provision of adequate moment arm length for the tail configuration. This length contributes to the CG travel by placing the propeller (a relatively large, fixed mass) farther from the cabin (the mass within which may vary substantially) than is typical for conventionally configured tractor airplanes. The forward baggage compartment of the pusher was incorporated specifically to provide the increased loading flexibility necessary to minimize the problem in practical operation.

Engine Installation

The study performance goals required a single, high-horsepower engine in each configuration. The GATP-1A study demonstrated the merits of using one high-output turboprop engine rather than two lower-output turboprops. The weight penalty for horsepower increases in turboprop engines of the power output class considered is extremely small compared to the weight growth of reciprocating engines, making it attractive to use a high-output engine. The engine selection was also influenced by projected cruise specific fuel consumption and by installation constraints. No unusual problems were encountered in the propulsion integration for any configuration, except as noted below. The -1B tractor installation was entirely straightforward, with a chin inlet and inertial separator as per manufacturer's data (ref. 4). The -2A uses an inlet and inertial separator mounted on the upper aft fuselage to avoid flow distortion due to inlet blanking in sideslip conditions. Experience with top-mounted jet fighter inlets has resulted in no flow problems with moderate angle of attack as long as the inlet face and location are carefully designed. The TPE 331-11 engine of the -1C configuration does not require an inertial separator inlet; however, its "straight-through" design necessitated an exhaust system incorporating a bifurcated duct to provide clearance for the nose landing gear installation. This "straight-through" engine arrangement prevented a TPE 331-11 pusher from being included in the study airplanes. There is no practical manner in which the TPE 331-11 could be installed backwards in the -2A configuration because of the engine's integral inlet and aft exhaust location. Adding additional gearing and shafting around the engine was not practical due to the complexity. The diesel pusher engine (-2D configuration) ingests both cooling and induction air through side-mounted inlets and exhausts the cooling air

8

through an annular exit around the spinner. The exhaust system and muffler exit beneath the fuselage in a conventional manner.

Undercarriage

The undercarriage arrangement differed between the configurations due to the differing wing positions. The tractor airplanes were configured with retractable tricycle landing gear with the main landing gear pivot points in the wings as per conventional practice. It was necessary to keep the stowed position of the gear as close to the wing roots as possible, because the small size of the wing provides marginal depth to house the strut, wheel, and tire. Since the turboprop pusher was configured as a mid-wing airplane, the main landing gear pivot points were located in the fuselage. This landing gear arrangement is similar to the high-wing, retractable-gear airplanes currently in production. The low wing of the diesel-powered pusher provided an opportunity for a wider track (a limitation of fuselage-mounted gear), therefore its main gear was moved to the wing. The track and wheelbase of each airplane were sized to satisfy FAR turnover angle requirements. Full-coverage landing gear doors were fitted to each configuration.

Wing

Wing planform definition for the study airplanes was based on a parametric study of aspect ratio and area variations to produce a cruise-matched wing. The cruise performance goals of the study required a minimum of excess wing area and a relatively high wing loading (approximately 35 lb/ft^2) for a general aviation airplane. An aspect ratio of 10 with a reference area of 120 ft^2 was chosen based on minimum area constraints defined both by FAR 23 stall speed requirements and internal fuel volume availability. The parametric study showed that while additional benefits could be gained with a wing aspect ratio of 12, the increase from aspect ratio 8 to aspect ratio 10 captured most of the gains due to higher aspect ratio, and obviated other problems such as further reduction in wing fuel volume and potential Reynolds number effects due to the very short chords that result. Fuel storage in the fuselage or in external tanks was considered an unacceptable solution to the fuel volume limitation problem. The wing was swept slightly forward (Λ_{LE} = -2°) in order to improve the spanwise flow characteristics. The taper ratio was set at 0.4 to keep the wing tip chord length

9

and Reynolds number from being undesirably small. Winglets were not considered due to the low cruise lift coefficient and relatively high aspect ratio of the wing. Wing twist (washout) was determined for elliptical span loading in cruise using a vortex-lattice analysis program (ref. 5). The twisted portion of the wing, which comprises only the outer 20 percent of the wing semispan, varies linearly from 0° to -2° total washout at the tip. In addition to approximating an elliptical loading, this washout should provide more acceptable airplane stall characteristics than an untwisted wing.

The NACA 65_2-415 airfoil section of the GATP-1A was replaced with a NASA-Langley developed section, designated NLF(1)-0215F (ref. 6). This airfoil was designed to promote natural laminar flow while retaining the favorable lift characteristics of the NASA low-speed airfoil family, and was specifically targeted for application to high performance general aviation aircraft. Lift performance of the NLF(1)-0215F section is not degraded by the loss of laminar flow, as can happen with other airfoils designed for extensive laminar flow. This provides an obvious safety benefit in actual operation, where some contamination of the wing surface is unavoidable due to insect debris, rain, or dust. The airfoil was designed for cruise operation with a flap deflection of -10°, which reduces the lift coefficient for minimum drag and provides some pitching moment alleviation to reduce trim drag.

The relatively small wing area and resulting high wing loading necessitated the same extensive use of high-lift devices as on the GATP-1A to meet the FAR 23.49 stall speed requirement of 61 kt for single-engine airplanes. The high-lift devices consist of 15 percent chord, full span leading edge slats, and 30 percent chord, 90 percent span single-slotted Fowler flaps. The trailing edge flaps should present no problems when used with NLF airfoils since the boundary layer is turbulent over the aft part of the airfoil. The maintenance of natural laminar flow across the wing-to-slat junction at the leading edge presented a problem since flow across a typical gap causes transition. Deletion of the slats would have meant a wing resize to approximately 170 ft^2, the additional drag of which negated any savings due to laminar flow when compared to the 120 ft^2 wing. A variable-camber leading edge without joints was considered unrealistic for this application due to its complexity and manufacturing cost. Previous laminar flow control research indicated that a forward-facing step discontinuity, as presented in figure 8, was less likely to cause boundary layer transition than either a gap

10

or aft-facing step; therefore, this arrangement was proposed as a solution to the slat installation problem. Unpublished data was subsequently obtained which indicated that this concept would work on an airplane of this type. It is anticipated that the laminar-tolerant step height and edge profile will be within normal manufacturing tolerance using production composite material construction techniques.

Roll control is accomplished with differential spoilers supplemented by 10 percent span ailerons to maintain control system linearity. The spoilers could be deployed simultaneously for glidepath control as well, but this capability was not analyzed. All flap and slat system tracks and brackets were assumed to be internal to the wing, and all control surface gaps were assumed to be sealed.

Empennage

Tail sizing for both the tractor and the pusher airframes drew from the -1A study, and was based on static and dynamic stability and control requirements. Additionally, the -2A tail design was based on protection of the aft-mounted propeller from ground strike in case of overrotation, and is of a type that should be very spin-resistant. As a large percentage of general aviation accidents (particularly those involving high performance aircraft) are stall/spin related, the latter feature should be highly desirable.

AERODYNAMIC ANALYSIS

The performance criteria for this study required that all the configurations designed have both a high cruise speed and good fuel efficiency. The use of natural laminar flow (NLF) airfoil technology and cruise-matched wing sizing appeared to be the best aerodynamic solution to achieving both of these diverse requirements. The present family of NASA-designed NLF airfoils (excluding the NACA 6-series) consists of two designs by Somers (refs. 6, 7), and, therefore, does not adequately define the effects of variations in camber and thickness on NLF airfoil characteristics. These two airfoils, designed for a speed range below that of this study, are relatively thick (15- and 17-percent) and highly cambered in order to achieve maximum lift coefficients comparable to those of the NASA low-speed series airfoils. Although these airfoils have high cruise lift

11

coefficients and large negative pitching moments, deflecting the trailing edge upward causes the pitching moments to be reduced and the lift coefficient range for minimum drag to be lowered. A 25 percent chord flap tested on the NLF(1)-0215F airfoil and deflected -10° reduces the lift coefficient for maximum lift-drag ratio to .6. The cruise lift coefficients for the study configurations range from .2 to .3 at maximum cruise altitude, considerably below the maximum lift-drag ratio lift coefficient. With reduced payloads the mismatch is much greater. In order to improve the cruise efficiency, the configuration would either have to fly higher (restricted by engine performance), use an NLF airfoil with less camber (not available at present), reduce the wing area (limited by fuel volume and FAR 23.49 requirements), or fly at a slower airspeed. The first three of these were not evaluated in this study because of the reasons listed. The cruise lift coefficients are, however, in the range of minimum drag, thus permitting high cruise speeds.

The lift characteristics were determined using the method presented in reference 8. This method assumes that all slots, gaps, and overlaps in the flap system have been optimized. The lift curves are presented in figure 9 for flap deflections of -10 degrees, 0 degrees, and 40 degrees. These flap settings are used for cruise, takeoff, and landing, respectively. Using the maximum trimmed lift coefficient of 3.05, a minimum stall speed of 58.3 kt can be obtained for the GATP-2A configuration, which is 2.7 kt below the FAR 23 requirement. The other configurations have similar stall speeds.

Drag polars were constructed for the takeoff, cruise, and landing modes of flight. The drag was defined as:

$$C_D = C_{D_{P_{min}}} + \Delta C_{D_p} + C_{D_i} + C_{D_{trim}} + C_{D_{power}} + C_{D_{cooling}}.$$

The minimum value of parasite drag ($C_{D_{P_{min}}}$) consists of skin friction, profile, interference, roughness, and excrescence drag. Numerical models of both basic airframes were developed for input into wetted area and skin friction computer codes. Form factors to account for thickness effects were obtained from reference 8. Skin friction coefficients were calculated for both turbulent and mixed laminar/turbulent boundary layers depending on the configuration. Laminar flow was assumed to exist on 60 percent of the wing lower surface and 40 percent

12

of the wing upper surface, the design transition locations of the airfoil. Laminar flow was assumed to exist on 20 percent of the tail areas on all configurations, and 10 percent of the fuselage wetted area on the pusher configurations (approximately from the nose to the windshield junction). Excrescence and interference drag increments were calculated using the data of reference 9. Flush-mounted antennae and a minimum of protuberances were assumed to exist. Parasite drag was increased three percent to account for roughness effects, as opposed to the five percent increment added to the GATP-1A analysis. This difference was intended to account for the improved surface finish available with composite structure rather than riveted aluminum.

The VORLAX computer program (ref. 5) was used to obtain the induced drag (C_{D_i}), with the percentage of leading edge suction having been determined using the method of reference 10. The variation of parasite drag with lift (ΔC_{D_p}), which included angle-of-attack dependent friction drag, pressure drag, and the effects of a non-elliptical load distribution on the wing, was determined using an unpublished method based on correlations with flight data.

Trim drag $(C_{D_{trim}})$ was calculated for an average center of gravity position and applied as an increment to the cruise drag polar. Trim drag was considered negligible for the takeoff mode of flight; however, a trimmed drag polar was used in calculation of the landing performance due to the importance of trimmed lift coefficient on the approach speed.

Power effects on lift and drag $(C_{D_{power}})$ were calculated using the methods of reference 8. While power effects on lift and drag are small for cruise conditions, they are large during takeoff, where the components of the airplane immersed in the propeller slipstream experience a much higher velocity than those in the freestream. The effects of power were much smaller for the pusher configurations than for the tractor configurations since no airframe components are located in the pusher propwash. The increment in drag at the cruise condition was added to the polar. Since approaches are usually made at low power settings, no power effects on lift or drag were included in the landing analysis.

All cooling drag $(C_{D_{cooling}})$ for the turboprop configurations is accounted for in the engine performance data except for the PT6A-45A oil cooler airflow, for which an increment was added to the parasite drag. The TPE-331-11

does not require an externally-mounted oil cooler. The cooling airflow requirement and cooling drag of the -2D configuration were calculated with the method presented in reference 11. Although the cooling airflow for the diesel engine is not large compared to that of a conventional reciprocating engine, the cooling drag amounted to 20 percent of the airplane minimum drag at an average cruise condition.

Lift and drag increments for the high-lift devices were determined using the methods of reference 8. Landing gear drag ($\Delta C_{D_{gear}}$ = .0394) was calculated using the method of reference 9, but is not included in the drag polars presented. Typical cruise, takeoff, and landing polars are presented in figures 10, 11, and 12, respectively. Tabulated cruise polar data for all of the study configurations are presented in Appendix A. Figures 13 through 17 present the average cruise lift-drag ratios as a function of cruise airspeed. From these plots it can be seen that in order to fly at high speeds and still retain a reasonable lift-drag ratio, cruise segments must be flown at as high an altitude as possible.

PROPULSION ANALYSIS

Engines

Three different engines were examined in this study: the Pratt and Whitney Aircraft of Canada PT6A-45A, the Garrett Airesearch TPE 331-11, and a Teledyne Continental conceptual diesel engine. The two turboprop engines represent currently available propulsion technology, while the diesel engine represents near-term (5 to 10 years) advanced technology. The basic geometry and dimensions of the three engines may be seen in figure 18.

The Pratt and Whitney Aircraft of Canada PT6A-45A is a free turbine, axial-plus-centrifugal compressor turboprop engine equipped with an integral reduction gearbox. The PT6A-45A was certificated in February, 1976; however, the basic design of the PT6 series of engines dates back to 1959. The PT6A-45A engine performance data used in this study was originally generated for the GATP-1A study with the aid of a computer program supplied by the manufacturer. For this study it was decided to flat rate the engine to 900 shp of its available 1,173 shp to

provide more consistent airplane performance in high density altitude situations. Installation penalties including inlet ram recovery, pressurization bleed airflow, and accessory power extraction were accounted for in the engine performance calculations as listed in table III. Engine data could not be generated above 30,000 ft due to computer program constraints, therefore it was necessary to extrapolate the data to 35,000 ft to adequately define the desired airplane flight envelope.

The Garrett Airesearch TPE 331-11 is a single-shaft turboprop engine equipped with an integral reduction gearbox. The TPE 331-11 was certificated in 1979, but its basic design dates back to the early 1960's. Performance data for this engine was supplied by the manufacturer, and included the same bleed air and accessory power extraction installation penalties as for the PT6A-45A (see table III). The TPE 331-11 has a rating of 1,000 shp dry, or 1,100 shp with water/alcohol injection, but was flat rated at 900 shp for this study. The TPE 331-11 was included in this study primarily because performance data was available to 45,000 ft, allowing an investigation of airplane performance at higher altitudes than possible with the PT6A-45A engine data. No attempt was made to compare the turboprop engines per se, nor was any intended.

The Teledyne Continental conceptual diesel engine data used in this study was supplied in part by the NASA-Lewis Research Center and was also derived from references 11 and 12. The subject engine is a six-cylinder, turbocharged, two-stroke diesel, with the cylinders radially disposed in two banks of three each. The study engine was rated at 500 shp, and had a turbocharger critical altitude of 17,000 ft. It was originally intended to obtain a diesel engine with high altitude (i.e., above 20,000 ft) performance comparable to the turboprop, but no such design was available. Scaling the available data up to the desired power rating was not possible due to thermodynamic cycle and physical size considerations. Increasing the critical altitude of the turbocharger was not possible for the same reasons, leaving the 500 shp engine as the only realistic choice. Additional data on the diesel engine is presented in table III.

Propeller Selection

Propeller selection and performance calculations were accomplished with the aid of a computer program based on the Hamilton Standard methods of reference 13.

15

These methods are based on the systematic variation of basic propeller geometric and aerodynamic design parameters over the desired range of operating conditions, allowing an optimum propeller to be selected. A parametric analysis using each set of engine data resulted in the definition of two different basic propellers, the characteristics of which are listed in table IV. The turboprop versions use pusher or tractor four-bladed, 90 inch diameter propellers, while the diesel uses a three-bladed, 90 inch diameter pusher propeller of lower activity factor due to its lower power output. All propellers were assumed to be of composite construction. It was also assumed that the pusher driveshaft could be developed using technology derived from current helicopter and airplane designs.

Propeller efficiency varied as a function of airspeed, altitude, and power setting. Corrected propeller efficiencies approached 0.90 for the turboprops and 0.92 for the diesel in the cruise condition. A representative plot of the efficiency variation with flight condition is presented in figure 19. The propulsion data used in the turboprop airplane performance calculations included the thrust contribution from the engine exhausts. Propeller reverse thrust performance was not analyzed, although this capability would be made available in a production airplane.

WEIGHTS ANALYSIS

Estimated weights for the study airplanes were calculated using empirical techniques presented in reference 14 and manufacturers' data wherever possible. A comparison of the study airplane weight summaries appears in table V. For the purpose of maintaining conventional weights engineering terminology, the weight of the pilot and his baggage was included in the operating weight empty.

An important point became apparent during an examination of wing weight variation with airfoil thickness ratio. For wings such as those of the study aircraft (low sweep, moderately high aspect ratio, and equipped with both leading and trailing edge devices) the wing weight is relatively insensitive to thickness ratio (fig. 20). This is because the basic wing in such a design serves mainly as a box to which the high-lift devices are attached. The ability to decrease thickness ratio without a large increase in wing weight for this airplane is very

desirable, particularly from an aerodynamic standpoint. A decrease in airfoil thickness ratio would reduce available fuel volume slightly, but would also net a decrease in drag and corresponding increase in cruise performance.

Use of the empirical weight estimation techniques required certain assumptions as to the structural design of the aircraft. All study airplanes were assumed to be constructed of fiber reinforced composite materials in a manner which takes optimum advantage of the material properties. This was necessary to realize the full amount of potential weight reduction due to composite construction. It was assumed that the structures would consist mainly of Kevlar*/epoxy skins over Nomex* honeycomb cores, with graphite/epoxy reinforcement in high compressive stress areas. Conventional skin/stringer structural design, as incorporated in the aluminum GATP-1A and most current airplanes, does not take full advantage of composite material properties. Kevlar was chosen as the basic structural fiber because of physical properties superior to fiberglass and cost lower than graphite. Kevlar offers high impact and abrasion resistance, and is unique among popular fiber reinforcements in its ability to deform plastically rather than failing catastrophically when its elastic limit is exceeded. No strict identification was made of a matrix material other than to specify it as epoxy (rather than polyimide, for example) because of the large variety of resin systems available. The weights of these resin systems are roughly comparable, therefore such generalization is valid.

Weight savings credited to composite construction ranged from 15 to 30 percent depending on the particular airframe component. This resulted in a net airframe structural weight reduction of approximately 20 percent as compared to conventional aluminum construction. Although possessing the potential for adequate surface finish and some reduction in labor intensity, bonded metal construction was rejected based on its relatively small weight savings potential. Reference 15 indicates weight savings due to bonded metal of zero to 10 percent as compared to conventional construction. Other advanced or exotic structural materials such as boron fibers, aluminum-lithium, or titanium alloys were not examined based on cost and availability considerations.

---

*Trademark of E. I. DuPont de Nemours & Co., Inc.

PERFORMANCE ANALYSIS

Takeoff and Climb

The study objectives required takeoff distances of 2,500 ft or less over a 50 ft obstacle at sea level, standard day conditions and maximum gross weight for each configuration. Despite relatively high wing loadings, the study airplanes easily exceed this requirement due to their high thrust-weight ratios and resulting high accelerations. Figure 21 presents the takeoff distance over a 50 ft obstacle as a function of density altitude for the -2A and -2D configurations. The other turboprops in the study have approximately the same wing loading and thrust-weight ratio as the -2A, and would exhibit similar takeoff performance. As shown in figure 21, the -2A configuration is capable of departure from a 2,500 ft runway at maximum gross weight at density altitudes exceeding 8,000 ft; the -2D airplane is similarly capable to a density altitude of 6,600 ft. This capability would allow operation from nearly all airports at maximum gross weight and at temperatures well above standard day conditions.

The time, fuel, and distance for the climb segment of the mission for each study airplane are presented in figures 22, 23, and 24, respectively, for standard day conditions and design takeoff gross weight. All the turboprop configurations have comparable climb performance, while that of the diesel-powered -2D is lower due to its lower installed power. The -2D does, however, use from 23 to 30 percent less fuel. The corresponding rates of climb for each aircraft are presented in figure 25. Again the effects of power are apparent in the lower climb rate of the diesel airplane. The nearly constant rates of climb of the -1B, -2A and -2C configurations at low altitude are due to the flat rating of their PT6A-45A engines. This is also true of the -1C configuration, although it is not as pronounced due to its lesser power before flat rating. The climb performance of the turboprop airplanes is such that even for a relatively short-range flight it is most efficient to climb to maximum cruise altitude. An additional benefit of this climb performance is that it would allow the airplanes to more effectively interface with heavier traffic at large airports, and also allow them to have a considerably smaller noise footprint.

18

Cruise

The mission performance was calculated for cruise altitudes from 20,000 to 40,000 ft. Limitations on the engine data available prevented any analysis of the -1B, -2A, and -2C configuration above 35,000 ft and the -2D above 30,000 ft. The climb to cruise altitude was at the best rate of climb airspeed. Allowances for both fuel consumed and distance traveled during the climb and descent phases were included in the mission performance calculations.

The beneficial effects of using NLF were ascertained by comparing the performance characteristics of the geometrically identical -2A and -2C configurations (figs. 26 and 27). The -2A configuration was assumed to exhibit 50 percent NLF on the wings, 20 percent on the tail surfaces, and 10 percent on the fuselage, whereas the -2C configuration was assumed to have a fully turbulent boundary layer on all surfaces. The maximum cruise speed was increased from 338 to 360 kt at 20,000 ft by the presence of NLF, reflecting an 18 percent decrease in drag coefficient. A similar increase in cruise speed, from 321 kt to 345 kt, occurred at the design altitude of 35,000 ft. The fuel efficiencies at the design altitude and speed increased 16.9 percent, from 66.3 to 77.5 seat nautical miles per gallon (SMPG). The most economical cruise speed, which occurs at an altitude of 35,000 ft, increased from 260 kt to 272 kt with NLF and the corresponding peak fuel efficiency increased from 71.4 to 80.5 SMPG (fig. 28). These results also reflect the effects of the total loss of NLF during flight due to surface contamination by insects or other debris. Although no detailed performance analysis was conducted regarding the loss of NLF on the other configurations, similar decreases in performance and fuel efficiency would be expected due to their geometric similarity.

The net difference between the tractor and pusher configurations was small. The increased amount of laminar flow possible with a pusher configuration was offset by the increased wetted area required to install the engine behind the passenger compartment. The maximum speed of the -1B tractor configuration was 367 kt at 20,000 ft altitude (fig. 29), 7 kt faster than the equivalent -2A pusher configuration. At the design cruise conditions the difference in fuel efficiency was small: 78.9 SMPG for the -1B vs. 77.5 SMPG for the -2A. The speeds and fuel efficiencies at the most economical cruise conditions were also very close: 273 kt and 80.7 SMPG for the -1B, and 272 kt and 80.5 SMPG for the -2A.

19

The performance of the diesel-powered -2D airplane was superior to the turbo-prop configurations in the area of fuel efficiency, but could not match their speeds, climb rates, or cruise altitudes. The -2D performance was heavily influenced by the critical altitude of the turbocharger, above which the available engine power degrades rapidly. At 275 kt, its maximum cruise speed (fig. 30) was considerably lower than that of the turboprops, but it is still faster than most current twin-engine aircraft with similar load carrying capability. At its maximum altitude of 30,000 ft, the diesel configuration achieved a cruise speed of 247 kt and a corresponding fuel efficiency of 118.3 SMPG. Its most economical cruise conditions were 154 kt at 20,000 ft altitude, yielding a fuel efficiency of 139.5 SMPG, 73 percent greater than the best of the turboprop airplanes. The operating characteristics of the diesel engine dominated the performance characteristics of the -2D and tended to force it to fly at lower altitudes for greater engine efficiency. Flying at these lower altitudes caused the airplane to operate at a lift coefficient below optimum and therefore at a much lower lift-drag ratio, as discussed earlier. This could have been alleviated to some extent by reducing the wing size of the -2D. Due to its lower fuel volume requirement and lower gross weight, the wing size reduction could be accomplished without violating either the fuel volume or approach speed constraints; however, no resizing was performed for this study.

In order to determine if additional performance gains could be achieved by flying the cruise segment of the flight profile at a higher altitude, the -1C configuration with a Garrett TPE 331-11 engine was developed. As shown in figure 31, the increase in altitude allowed only marginal gains in performance due to the rapid degradation of thrust with altitude. In going from an altitude of 35,000 to 42,000 ft, maximum range increased 6.3 percent from 1,312 to 1,400 n.mi. while maximum cruise speed decreased 20.6 percent from 340 to 270 kt. Similar trends could also be expected with the PT6A-45A powered configuration at higher altitudes. The maximum cruise speed of the -1C was 340 kt, 27 kt below the -1B configuration. Its maximum fuel efficiency at 35,000 ft (fig. 28) was also less than the -1B; 72.8 versus 81.2 SMPG. Although this value increased to 78.9 SMPG at 286 kt and 40,000 ft, flight at altitudes of 40,000 ft and above would be of marginal use because of the very small flight envelope available.

The cumulative effect of all the current advanced technology items addressed can be seen by a comparison of the -1A (fig. 32) with the -1B configuration.

Maximum cruise speed increased from 331 kt to 367 kt and the most economical cruise speed increased from 236 kt to 273 kt. The speed increase was accompanied by a 31 percent increase in fuel efficiency at the design cruise condition and a 24.7 percent increase at the most economical cruise condition. Although not having any speed advantage over the -1A configuration, the -2D configuration did have an increase in fuel efficiency of 96.5 percent at the design cruise condition and 115.6 percent at the most economical cruise condition.

In addition to the change in structural material in going from the -1A to the configurations of this study, changes were made in the aspect ratio, airfoil section, and propeller. This prevented any direct evaluation of the performance increase due to structural weight reduction, however, only small gains in performance can be expected from further decreases in weight. This is reflected in the range-payload plot (fig. 33). After the maximum fuel capacity point is reached only the -2D configuration gains any appreciable increase in range with reduction in weight. Because of its lower cruise speed, the -2D configuration operates in a lift coefficient range where the lift-drag ratio does not vary as greatly with lift as that of the turboprop powered configurations. As mentioned earlier, the configuration cruise lift coefficients are such that they occur at or near minimum drag. Therefore, any additional decrease in weight results in little or no decrease in drag, and a large decrease in lift-drag ratio.

Figure 34 (from ref. 16) presents the cruise specific range of a large number of general aviation and business airplanes. Also plotted on this figure are the results from the study of reference 1 and the present study. The turboprop powered GATP series of configurations fall into a group which illustrates the performance and fuel conservation advantages of the study configurations. Compared to current reciprocating-engined twins, the study turboprops exhibited a cruise speed advantage of over 130 kt for roughly comparable specific range performance. Compared to turboprop-powered twins with comparable cruise speeds, the study turboprops exhibited specific range performance which was approximately three times better. Cruise speed and specific range of the diesel-powered airplane differed substantially from those of the turboprop study airplanes. Although its maximum cruise speed was 120 kt slower than that of the turboprops, the diesel-powered airplane's specific range performance was twice that of the turboprops; it also offered three times the specific range performance of current reciprocating-engined twins at comparable cruise speed.

Landing

The landing performance of the -2A configuration is presented in figure 40 for a combination of landing weights and density altitudes. Since all the configurations are aerodynamically similar in the high-lift mode of flight, the landing performance of only the -2A configuration was analyzed. The landing distances presented in figure 35 are in the same range as the takeoff distances of figure 25. The short landing distance is a result of the use of an extensive high lift system and a low approach speed. The landing analysis was conducted assuming the use of spoilers to decrease lift and increase drag during the landing roll, but did not include propeller thrust reversing, which would result in a further landing distance reduction.

A summary of the performance data for all the configurations is presented in table VI.

Comparison with Similar Study

These results may be compared to those reported in reference 17. Although this technology-integration study was similar in many aspects, certain differences in assumptions and methodology are significant. Examples of these differences are the freedom in reference 17 to scale both wing area and propulsion system data and not be constrained by physical layout.

The study airplanes of reference 17 were developed using essentially the same baseline airplane and mission as the current study, but were resized for optimum cruise with successive technology improvements and were not constrained by the FAR 23.49 stall speed limit. Relaxation of the stall speed limit allowed deletion of the leading edge high-lift devices and provided more certainty of maintaining NLF on the wing, but resulted in stall speeds as high as 76 kt. The mismatch of airfoil characteristics noted in the current study was not a limitation in reference 17. The fuel usage penalty imposed by meeting the FAR 23.49 constraint ranged from 1.5 to 6.9 percent when comparing airplanes with both wing and engine sizes optimized for maximum cruise specific range against airplanes having wing loadings limited by FAR 23.49. No configuration layouts were presented in the alternate study and no wetted area penalty was assessed to the pusher configurations in reference 17, but a scrubbing drag reduction was credited.

22

Reference 17 examined turboprop and diesel engines which were considerably different from those studied here. The turboprop engine considered was the NASA General Aviation Turboprop Engine (GATE), with approximately 7 percent improved BSFC at cruise than the PT6A-45A or TPE 331-11. The diesel engine used was much larger than the one used in the current study, and was rated at 1,170 shp as opposed to 500 shp. Specific range performance of the diesel-powered airplanes slightly exceeded 3 n. mi./lb at comparable airspeeds in both studies. In addition to the above, reference 17 examined two additional engines: an advanced technology reciprocating engine and a liquid cooled rotary engine. The rotary engine proved to be the lightest and most fuel-efficient of the engines examined. The cooling drag of the liquid cooled rotary was reported to be zero, which contributed to its superior showing.

CONCLUDING REMARKS

Very substantial benefits can be gained from the application of currently available advanced technology to general aviation airplanes. Of the technologies examined, the application of natural laminar flow (with drag coefficient decreases on the order of 18 percent) produced the largest gains in performance and large increases in fuel efficiency. Greater benefits could have been realized if the airfoil characteristics had more closely matched the airplane cruise condition. A reduction in wing area would have helped achieve a better match, but internal fuel volume and stall speed requirements prevented this approach. The limited amount of data available on NLF airfoils precluded selection of a different airfoil section. For NLF technology to be fully exploited, aerodynamic data should be generated for a comprehensive series of NLF airfoils addressing variations in thickness and design lift coefficient. Extensive research remains to be done on the integration of high-lift devices, particularly leading edge devices, to this type of airfoil. The problem of keeping the NLF wing free of transition-inducing contamination from rain, ice, and insects is currently being addressed, but no clear solution is at hand.

The application of advanced diesel engine technology resulted in increases in fuel efficiency from 46 to 73 percent greater than the best of the turboprops at the expense of some decrease in cruise speed. The diesel engine analyzed is still several years away from the prototype stage, and was the only study technology not

23

immediately available. Even with the limited cooling requirements made possible by ceramic engine components, the cooling drag of the diesel engine was still 20 percent of the airplane minimum cruise drag. The limited power output and high lapse rate of the diesel engines of reasonable weight and size are also drawbacks when compared to turboprop engines. Many aspects of the diesel engine design and operation remain to be proven before the predicted efficiency of the engine can be utilized.

The benefits of composite structural materials and pusher configuration design on performance were not as great as anticipated. Much of the performance increase usually associated with the decrease in induced drag made possible by the reduced weight of composite structure (20 percent of structural weight) was offset by a profile drag increase due to the NLF airfoil characteristics; however, the weight savings and surface finish available with composite materials were still important and necessary in meeting other criteria. The increase in the amount of natural laminar flow on the pusher configurations as compared to the tractor configurations was offset by the pushers' greater wetted area. The pusher configurations were more sensitive to loading and balance, which may be an operational drawback. The interior noise level of the pusher airplanes would likely be lower than that of the tractor airplanes. Other operational aspects of the pusher configuration indicated no significant advantages over a conventionally configured airplane of this class.

The net result of the technology applications examined is apparent when the cruise speed and corresponding specific range figures for the study airplanes are compared with those of current airplanes. These configurations have cruise speeds equal to or greater than those of current twin turboprop-engined airplanes and specific ranges greater than current twin reciprocating-engined airplanes. Although the cruise speed of the diesel-powered -2D configuration is not as great as that of the current twin turboprop-engined airplanes it is equal to the speed of the fastest of the current twin piston-engined airplanes. The -2D configuration also has a specific range much greater than any comparable current airplane.

24

Appendix A

Tabulated Drag Polar Data

Cruise Condition, All Configurations

C_L	C_{D_i}
0	.0094
.05	.0067
.10	.0050
.15	.0036
.20	.0029
.25	.0027
.30	.0029
.35	.0037
.40	.0049
.45	.0067
.50	.0084
.55	.0107
.60	.0131
.70	.0187
.80	.0250
.90	.0321
1.00	.0398
1.10	.0490
1.20	.0575
1.30	.0669

GATP-1B

Minimum Drag Coefficients

ALTITUDE	MACH NUMBER					
	.1	.2	.3	.4	.5	.6
0	.02147	.01920	.01799	.01718	.01654	.01602
5000	.02197	.01958	.01834	.01752	.01687	.01632
10000	.02252	.02004	.01873	.01789	.01723	.01664
15000	.02307	.02050	.01920	.01827	.01757	.01699
20000	.02373	.02102	.01962	.01870	.01799	.01739
25000	.02438	.02159	.02012	.01911	.01843	.01781
30000	.02512	.02219	.02065	.01967	.01888	.01825
35000	.02492	.02282	.02124	.02020	.01936	.01870

GATP-1C

Minimum Drag Coefficients

ALTITUDE	MACH NUMBER					
	.1	.2	.3	.4	.5	.6
0	.02097	.01870	.01749	.01668	.01604	.01552
5000	.02147	.01908	.01784	.01702	.01637	.01582
10000	.02202	.01954	.01823	.01739	.01673	.01614
15000	.02257	.02000	.01870	.01777	.01707	.01644
20000	.02323	.02052	.01912	.01820	.01749	.01699
25000	.02388	.02109	.01962	.01861	.01793	.01731
30000	.02462	.02169	.02015	.01917	.01838	.01775
35000	.02442	.02232	.02074	.01970	.01886	.01820
40000	.02678	.02343	.02171	.02056	.01970	.01900
45000	.02808	.02454	.02264	.02143	.02052	.01978

GATP-2A

Minimum Drag Coefficients

ALTITUDE	MACH NUMBER					
	.1	.2	.3	.4	.5	.6
0	.02160	.01902	.01783	.01703	.01633	.01571
5000	.02213	.01949	.01824	.01736	.01664	.01602
10000	.02273	.01996	.01864	.01781	.01705	.01637
15000	.02330	.02044	.01911	.01825	.01748	.01682
20000	.02387	.02107	.01964	.01868	.01791	.01723
25000	.02477	.02166	.02010	.01910	.01833	.01768
30000	.02548	.02236	.02055	.01957	.01880	.01812
35000	.02614	.02309	.02101	.02005	.01928	.01861

GATP-2C

Minimum Drag Coefficients

ALTITUDE	MACH NUMBER					
	.1	.2	.3	.4	.5	.6
0	.02674	.02397	.02251	.02147	.02067	.02000
5000	.02735	.02446	.02296	.02190	.02109	.02039
10000	.02799	.02502	.02343	.02235	.02151	.02079
15000	.02866	.02558	.02396	.02283	.02197	.02123
20000	.02939	.02620	.02450	.02338	.02246	.02170
25000	.03018	.02687	.02511	.02393	.02299	.02221
30000	.03103	.02759	.02576	.02452	.02356	.02276
35000	.03198	.02837	.02698	.02518	.02417	.02335

GATP-2D

Minimum Drag Coefficients

ALTITUDE	MACH NUMBER					
	.1	.2	.3	.4	.5	.6
0	.02520	.02262	.02143	.02063	.01993	.01931
5000	.02573	.02309	.02184	.02096	.02024	.01962
10000	.02633	.02355	.02224	.02141	.02065	.01997
15000	.02690	.02404	.02271	.02185	.02108	.02042
20000	.02747	.02467	.02324	.02228	.02151	.02083
25000	.02837	.02526	.02370	.02270	.02193	.02128
30000	.02908	.02596	.02415	.02317	.02240	.02172
35000	.02974	.02669	.02461	.02365	.02288	.02221

THIS PAGE
INTENTIONALLY
LEFT BLANK

REFERENCES

1. Martin, G. L.; Everest, D. L.; Lovell, W. A.; Price, J. E.; Walkley, K. B.; and Washburn, G. F.: Design and Analysis of a Fuel-Efficient, Single-Engine, Turboprop-Powered Business Airplane, NASA Contractor Report 165768, August 1981.

2. Airworthiness Standards: Normal, Utility, and Aerobatic Category Airplanes. Federal Aviation Regulations, Volume III, Part 23, Federal Aviation Administration, June 1974.

3. Anthropometric Source Book, Volume I: Anthropometry for Designers. NASA Reference Publication 1024, July 1978.

4. PT6A-40 Series Installation Handbook. Pratt and Whitney Aircraft of Canada, Ltd., revised March 1977.

5. Miranda, Luis R.; Elliott, R. D.; and Baker, W. M.: A Generalized Vortex Lattice Method for Subsonic and Supersonic Flow Applications. NASA Contractor Report 2865, 1977.

6. Somers, Dan M.: Design and Experimental Results for a Flapped Natural-Laminar-Flow Airfoil for General Aviation Applications. NASA Technical Paper 1865, June 1981.

7. Somers, Dan M.: Design and Experimental Results for a Natural-Laminar-Flow Airfoil for General Aviation Applications. NASA Technical Paper 1861, June 1981.

8. U. S. Air Force Stability and Control DATCOM. Air Force Flight Dynamics Laboratory, revised April 1978.

9. Hoerner, S. F.: Fluid Dynamic Drag. Hoerner Fluid Dynamics, Brick Town, New Jersey, 1965.

10. Carlson, H. W.; and Walkley, Kenneth B.: A Computer Program for Wing Subsonic Aerodynamic Performance Estimates Including Attainable Thrust and Vortex Lift Effects. NASA Contractor Report 3515, March 1982.

11. Brouwers, Alex P.: 150 and 300 kW Lightweight Diesel Aircraft Engine Design Study. NASA Contractor Report 3260, April 1980.

12. Brouwers, Alex P.: 186 kW Lightweight Diesel Aircraft Engine Design Study. NASA Contractor Report 3261, April 1980.

13. Generalized Method of Propeller Performance Estimation. Hamilton Standard Division of United Aircraft Corp., Report PDB 6101, Revision A, June 1963.

14. Nicolai, Leland M.: Fundamentals of Aircraft Design. METS, Inc., Xenia, Ohio, 1975.

15. Kraus, E. F.; Mall, O. D.; Awker, R. W.; and Scholl, J. W.: Application of Advanced Technologies to Small, Short-Haul Transport Aircraft (STAT). NASA Contractor Report 152362, November 1982.

16. Holmes, B. J.: Aerodynamic Design Optimization of a Fuel-Efficient High Performance, Single-Engine, Business Airplane. AIAA Paper 80-1846, August 1980.

17. Kohlman, D. L.: Performance Improvements of Single-Engine Business Airplanes by the Integration of Advanced Technologies. DGLR Paper 82-064, October 1982.

TABLE I. – COMPARISON OF CURRENT STUDY SPECIFICATIONS WITH THOSE FOR THE STUDY OF REFERENCE 1.

Study Airplane	-1A	-1B, -1C, -2A, -2C, -2D
Cruise Performance		
Speed	>300 kt	Comparable to -1A
Altitude	>30,000 ft	Comparable to -1A
Range	1,300 n.mi.	1,300 n.mi.
Payload	1,200 lbs	1,200 lbs
Takeoff/Landing Performance		
Takeoff distance	≤2,500 ft	≤2,500 ft
Landing distance	≤2,500 ft	≤2,500 ft
Configuration		
Type(s)	Tractor	Pusher and Tractor
Pressurization	8,000 ft cabin @ service ceiling	8,000 ft cabin @ 35,000 ft
Construction	Aluminum	Composite
Aspect ratio	8	≥10
Sweep, .25c	0°	Forward
Certification	FAR 23	FAR 23

33

TABLE II. – CONFIGURATION GEOMETRY COMPARISON.

Overall Geometry		-1A	-1B	-1C	-2A(-2C)	-2D
Length	(ft)	33.56	37.25	36.75	38.08	38.08
Span	(ft)	30.80	34.64	34.64	34.64	34.64
Height	(ft)	10.35	11.25	11.25	11.33	11.33

Wing

Reference area (ft^2)		120	120	120	120	120
Span	(ft)	30.80	34.64	34.64	34.64	34.64
Aspect ratio		8.0	10.0	10.0	10.0	10.0
Taper ratio		0.33	0.40	0.40	0.40	0.40
Sweep, leading edge (deg)		3.6	-2.0	-2.0	-2.0	-2.0
.25c	(deg)	0	-4.5	-4.5	-4.5	-4.5
Mean aerodynamic chord (ft)		4.20	3.71	3.71	3.71	3.71
Thickness-to-chord ratio		.15	.15	.15	.15	.15
Dihedral	(deg)	3.0	3.0	3.0	3.0	3.0
Airfoil section		65$_2$-415	NLF(1)-0215F	NLF(1)-0215F	NLF(1)-0215F	NLF(1)-0215F

Fuselage

Length	(ft)	32.0	36.75	36.25	35.08	35.08
Width	(ft)	56	56	56	56	56
Height	(in)	65	65	65	65	65
Cabin length	(ft)	12.13	15.25	15.25	12.92	12.92
Cabin width	(in)	51	51	51	51	51
Cabin height	(in)	56	56	56	56	56

Horizontal Tail

Area	(ft^2)	29.0	33.0	33.0	41.7	41.7
Span	(ft)	11.42	13.0	13.0	12.50	12.50
Aspect Ratio		4.5	5.1	5.1	3.7	3.7
Taper ratio		0.7	0.56	0.56	0.6	0.6
Sweep, leading edge (deg)		6	0	0	15	15
Airfoil section		0009	0009	0009	0009	0009

TABLE II. - CONFIGURATION GEOMETRY COMPARISON (CONCLUDED).

Vertical Tail (Upper/Lower)

Area (total) (ft^2)	19.25	20.0	20.0	10.0/14.0	10.0/14.0
Span (ft)	5.0	4.9	4.9	2.5/3.5	2.5/3.5
Aspect ratio	1.3	1.3	1.3	1.25/1.75	1.25/1.75
Taper ratio	0.5	0.39	0.39	0.6/0.6	0.6/0.6
Sweep, leading edge (deg)	40	50	50	39/30	39/30
Airfoil section	0009	0009	0009	0009	0009

Propulsion

Engine	PT6A-45A	PT6A-45A	TPE 331-11	PT6A-45A	Diesel
Configuration	Tractor	Tractor	Tractor	Pusher	Pusher
Propeller diameter (in)	84	90	90	90	90
Blades	4	4	4	4	3

TABLE III. - ENGINE PARAMETERS FOR STUDY AIRPLANES.

Engine		PT6A-45A
Shaft horsepower		900
Type		Gas Turbine
Inlet ram recovery		.98
Service airbleed	(lbm/s)	.25
Accessory power extraction	(hp)	10
Propeller speed	(rpm)	1,700
Exhaust nozzle area	(in^2)	90
Fuel requirement		Jet A
Dry weight less accessories	(lb)	423

Engine		TPE 331-11
Shaft horsepower		900
Type		Gas Turbine
Service airbleed	(lbm/s)	.25
Accessory power extraction	(hp)	10
Propeller speed	(rpm)	1,591
Fuel requirement		Jet A
Dry weight less accessories	(lb)	400

Engine		Teledyne Continental Diesel
Shaft horsepower		500
Type		Reciprocating
Cycle		Two-stroke, turbocharged
Cylinders		6
Propeller speed	(rpm)	1,778
Cooling system		Air
Fuel requirement		Jet A
Dry weight less accessories	(lb)	500

TABLE IV. - PROPELLER PARAMETERS.

Airplane		-1A	-1B	-1C	-2A(-2C)	-2D
Diameter	(in)	84	90	90	90	90
Blades		4	4	4	4	3
Activity factor		180	140	140	140	100
Integrated C_L		0.5	0.5	0.5	0.5	0.5
Construction		Aluminum	Composite	Composite	Composite	Composite
Weight	(lb)	178	164	164	164	120
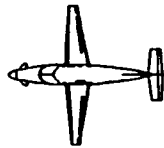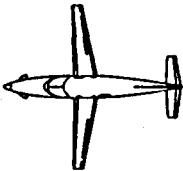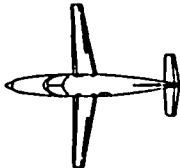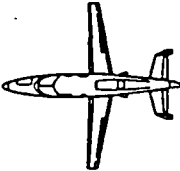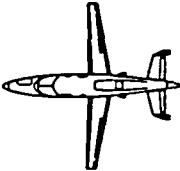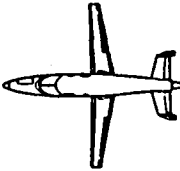
TABLE V. - STUDY AIRPLANE WEIGHTS SUMMARY COMPARISON.

Note: All weights shown in pounds.

Airplane	-1A	-1B	-1C	-2A(-2C)	-2D
Structure, Less Wing	990	814	809	779	814
Wing	410	300	300	300	300
Engine, Accessories, Propeller, and Drive	423 207	423 193	400 186	423 252	500 195
Systems	490	494	494	519	548
Weight Empty	2,520	2,224	2,189	2,273	2,357
Operating Items (Pilot and Baggage)	200	200	200	200	200
Operating Weight Empty	2,720	2,424	2,389	2,473	2,557
Passengers, 5	850	850	850	850	850
Baggage	150	150	150	150	150
Zero Fuel Weight	3,720	3,424	3,389	3,473	3,557
Mission Fuel	1,010	742	894	752(855)	447
Takeoff Gross Weight	4,730	4,166	4,283	4,225(4,328)	4,004

TABLE VI. - PERFORMANCE SUMMARY COMPARISON.

	GATP - 1A	GATP - 1B	GATP - 1C	GATP - 2A	GATP - 2C	GATP - 2D
AIRFOIL/ASPECT RATIO	65_2 - 415 / 8	NLF(1)-0215 F / 10	NLF(1)-0215 F / 10	NLF(1)-0215 F / 10	NLF(1)-0215 F / 10	NLF(1)-0215 F / 10
BOUNDARY LAYER	100% TURBULENT	50% LAMINAR WING	50% LAMINAR WING	50% LAMINAR WING 10% LAMINAR FUSELAGE 20% LAMINAR TAILS	100% TURBULENT	50% LAMINAR WING 10% LAMINAR FUSELAGE 20% LAMINAR TAILS
MAXIMUM CRUISE SPEED @ 35,000 FT	312 Kt	353 Kt	333 Kt	345 Kt	321 Kt	247 Kt @ 30,000 Ft
AVERAGE CRUISE L/D @ 300 Kt AND 35,000 FT	12.1	14.7	14.9	14.5	12.2	14.0 *
SEAT MILES PER GALLON @ 300 Kt AND 35,000 FT	60.2	78.9	72.14	77.5	66.3	118.3 *
MAXIMUM CRUISE SPEED/ALTITUDE	331 Kt/20,000 Ft	367 Kt/20,000 Ft	340 Kt/25,000 Ft	360 Kt/20,000 Ft	338 Kt/20,000 Ft	275 Kt/20,000 Ft
MOST ECONOMICAL CRUISE SPEED/ALTITUDE/SMPG	236 Kt/35,000 Ft/ 64.7	273 Kt/35,000 Ft/ 80.7	286 Kt/40,000 Ft/ 78.9	275 Kt/35,000 Ft/ 80.5	260 Kt/35,000 Ft/ 71.4	154 Kt/20,000 Ft/ 139.5

*247 Kt @ 30,000 Ft

THIS PAGE
INTENTIONALLY
LEFT BLANK

NOTE: All dimensions in feet unless otherwise specified.
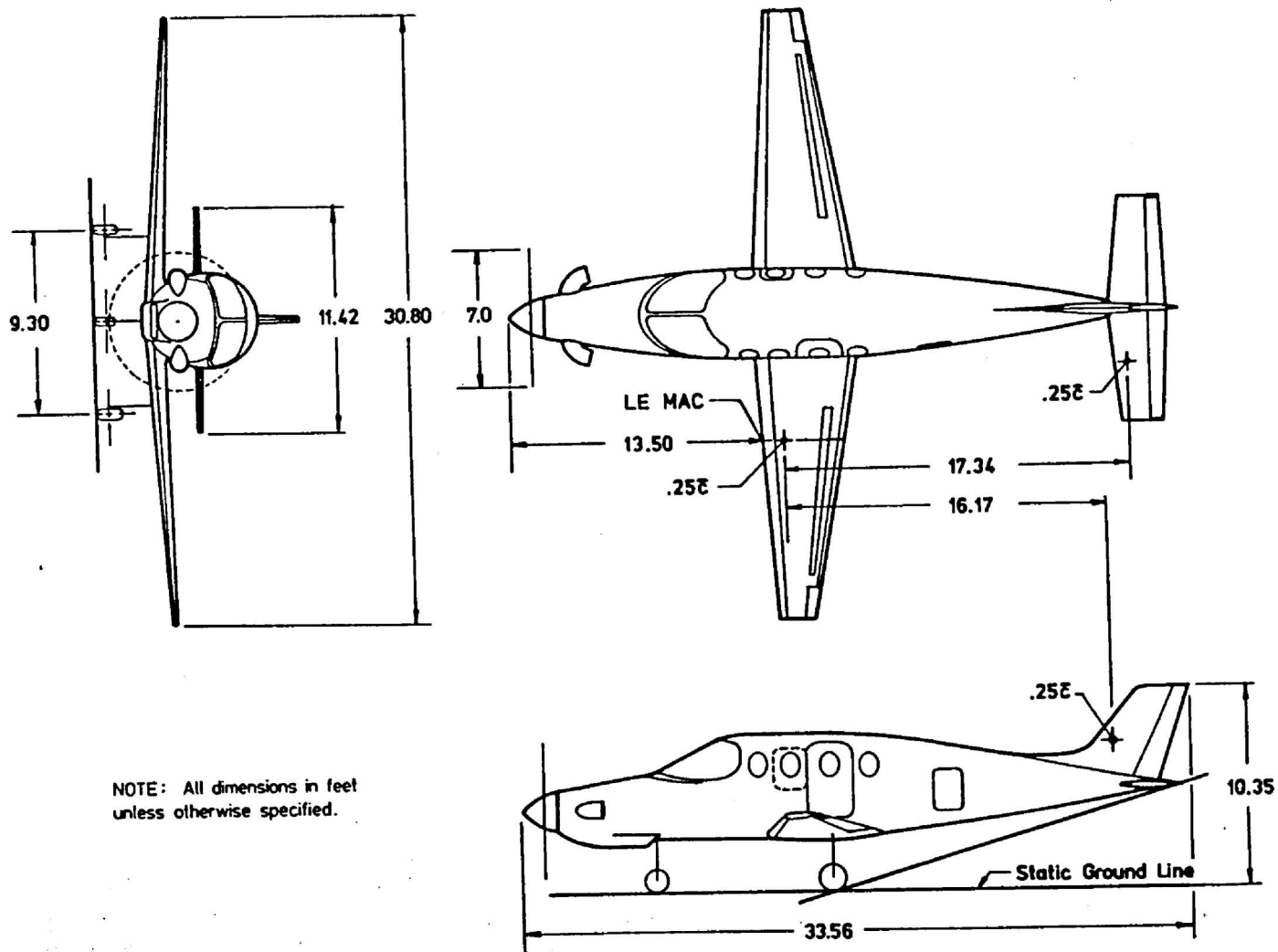
Figure 1. - GATP-1A general arrangement.

11.67

12.92 34.64

7.50

LE MAC

14.58

.25c̄

.25c̄

18.83

18.25

.25c̄

11.25

17°

Static Ground Line

37.25

NOTE: All dimensions in feet unless otherwise specified.
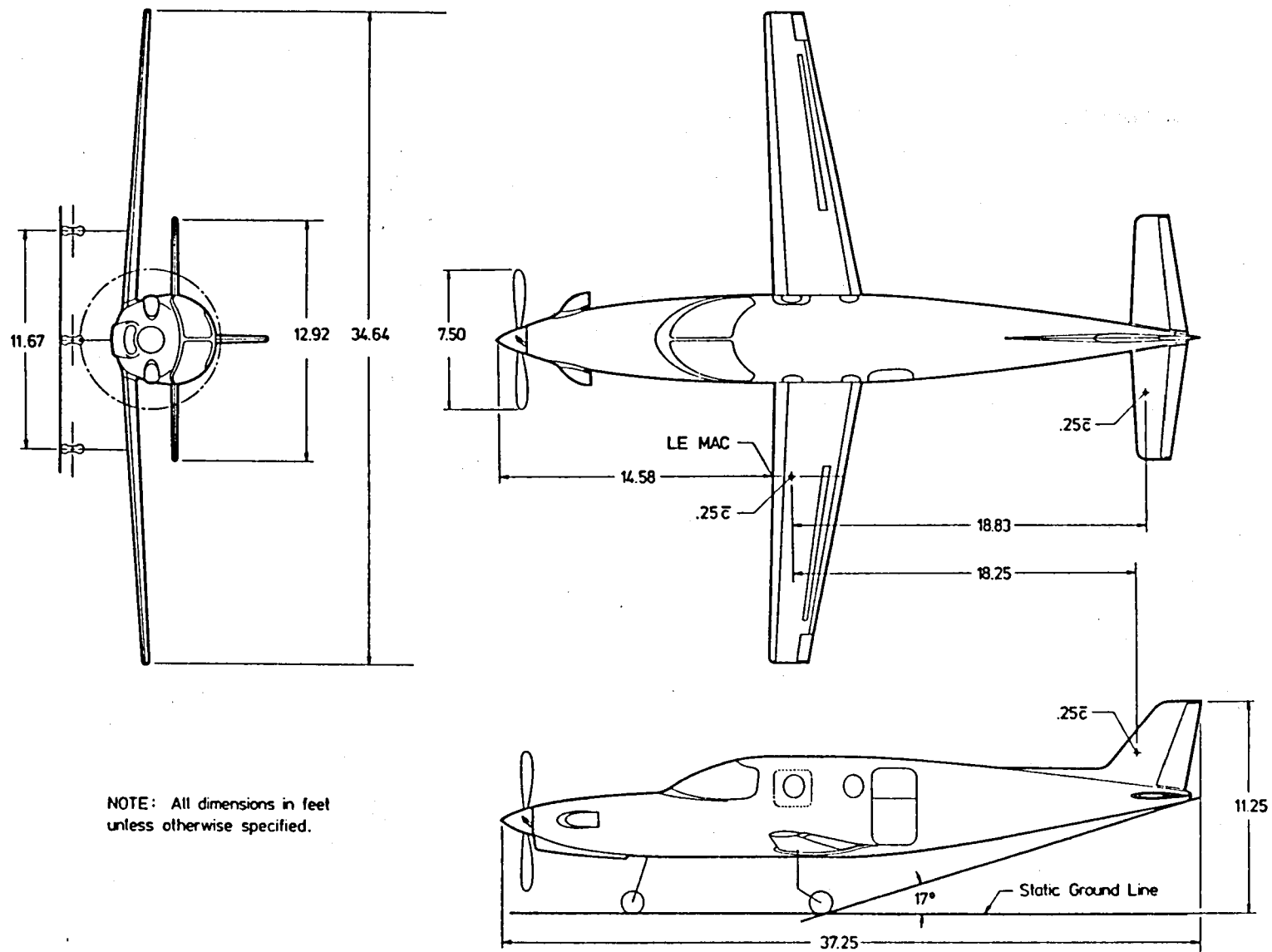
Figure 2. - GATP-1B general arrangement.

NOTE: All dimensions in feet
unless otherwise specified.

11.67   12.92   34.64

7.50

LE MAC
14.08
.25c̄
18.83
18.25
.25c̄

Garrett TPE 331-11 engine
.25c̄
11.25
Exhaust   17°   Static Ground Line
36.75
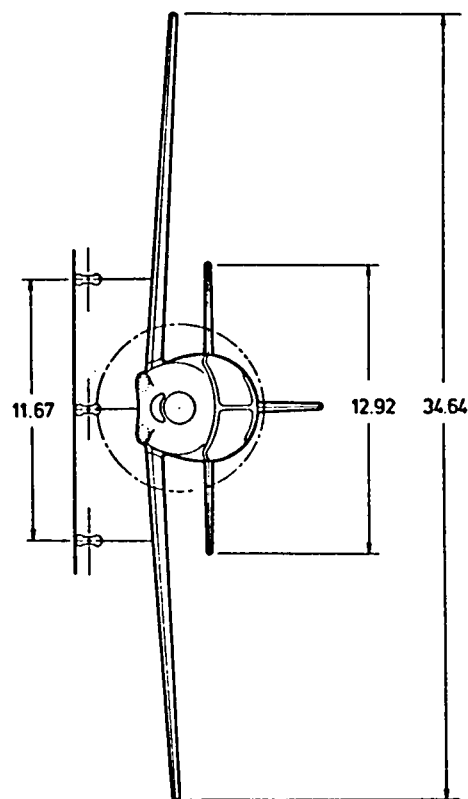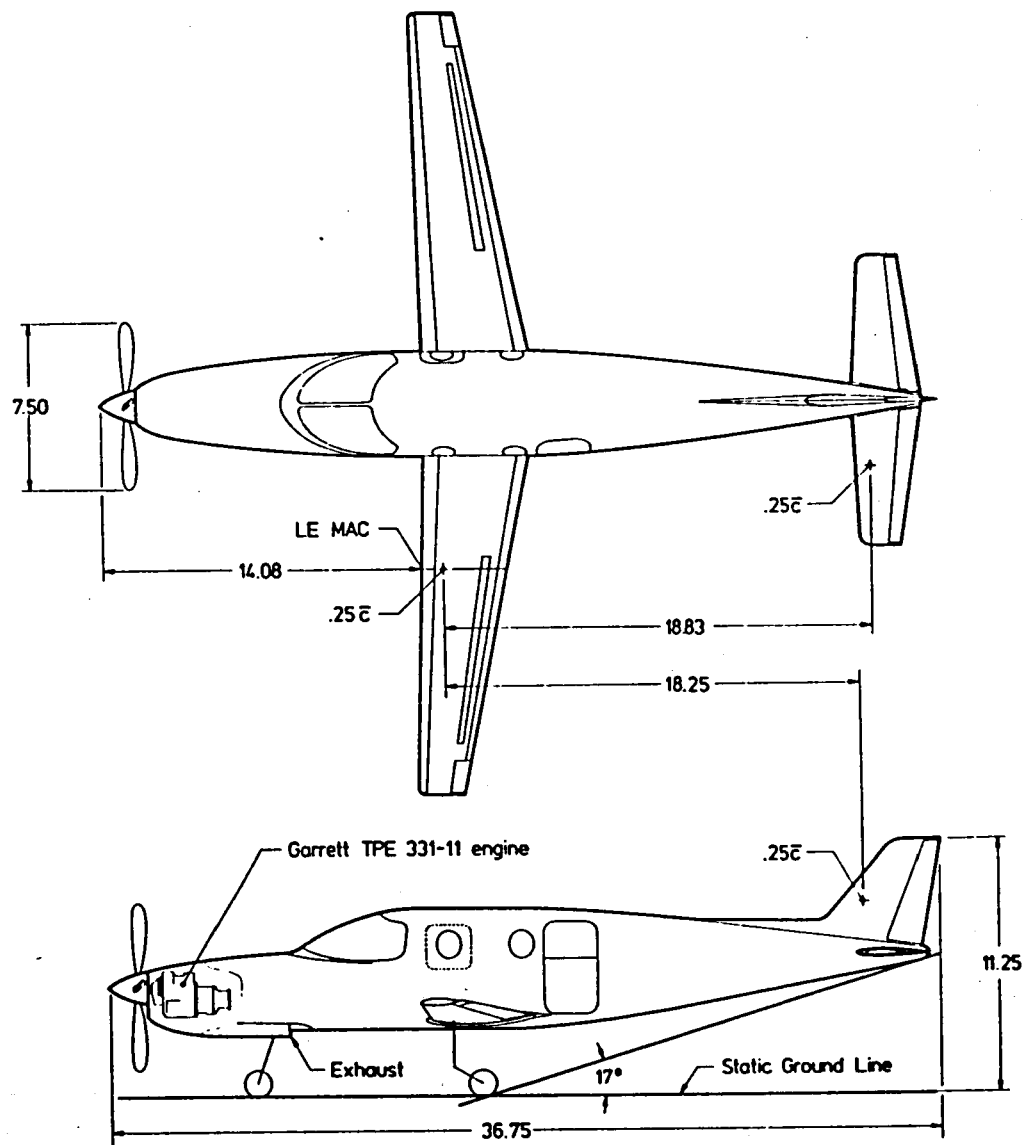
Figure 3. - GATP-1C general arrangement.

8.33

12.50   34.64

NOTE: All dimensions in feet
unless otherwise specified.

7.50

LE MAC

.25c̄

18.10

.25c̄

13.00

14.58

11.33

.25c̄

Static Ground Line

13°

38.08

Figure 4. - GATP-2A (-2C) general arrangement.
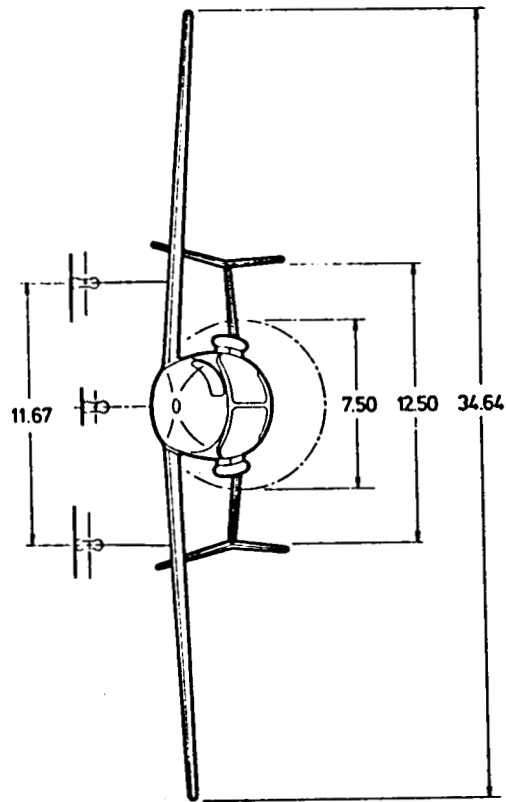
NOTE: All dimensions in feet unless otherwise specified.
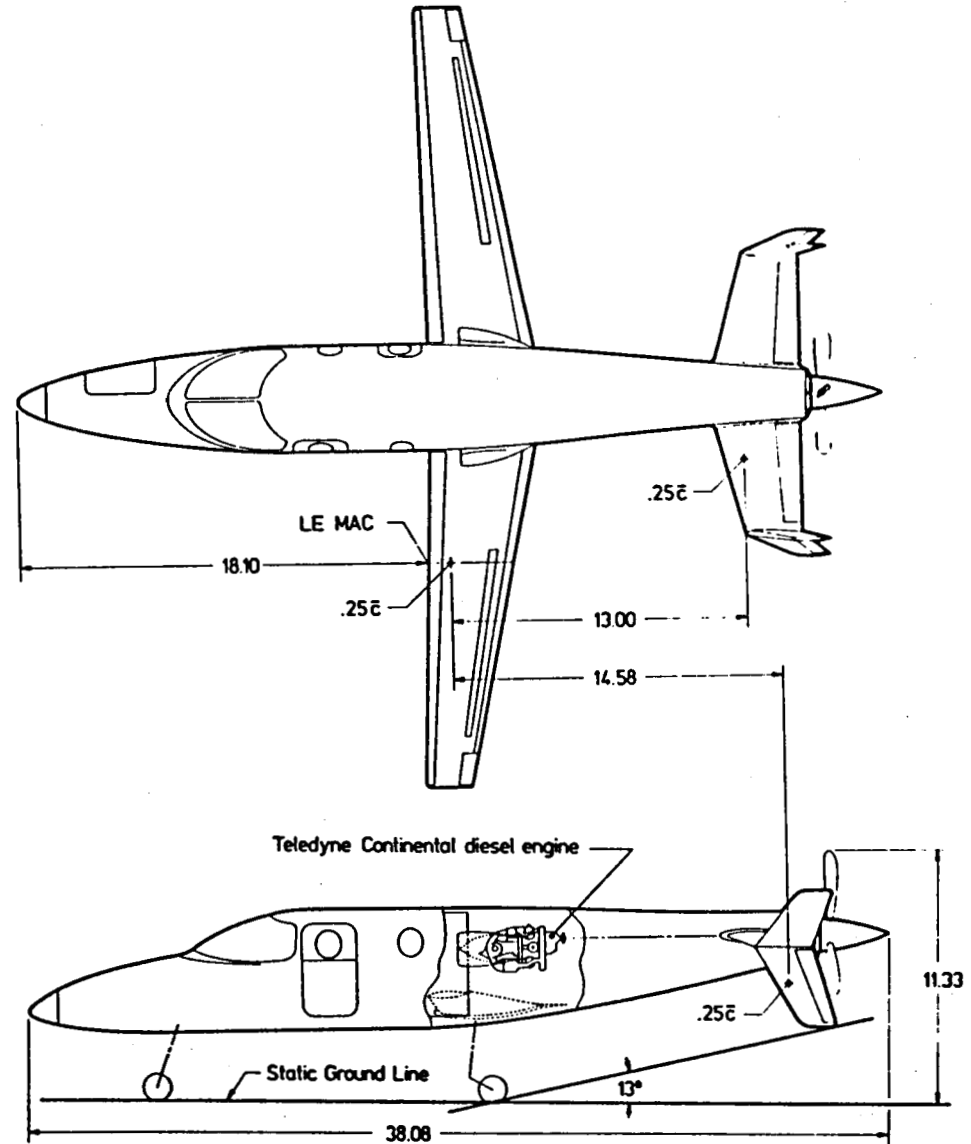
Figure 5. - GATP-2D general arrangement.

Slat tracks   Flap tracks

Aileron

NOTE: All dimensions in inches unless otherwise specified.

Front spar   Rear spar
Section B-B

Flap

Slat

Spoiler

Hyd. and elec. systems

Emergency exit

Baggage area

Environmental control system

60 gal fuel

Retracted MLG position

B   B

15 gal fuel

56
51
56   65
9

Section A-A

P&WAC PT6A-45A

Avionics

187

A

A

Inlet   40   A   Cabin door
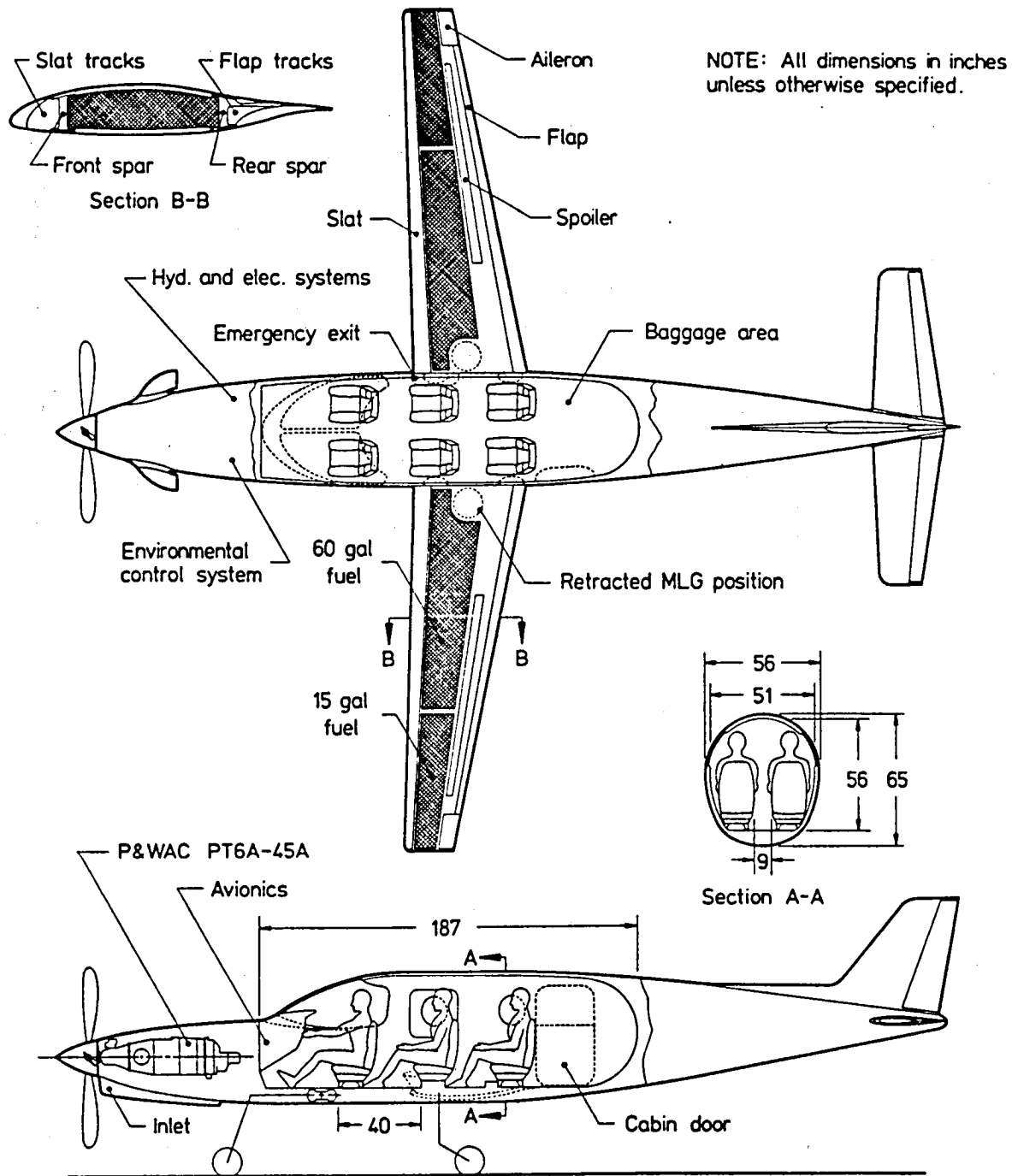
Figure 6. – GATP-1B interior arrangement.

46

Section B-B

Section A-A

NOTE: All dimensions in inches unless otherwise specified.
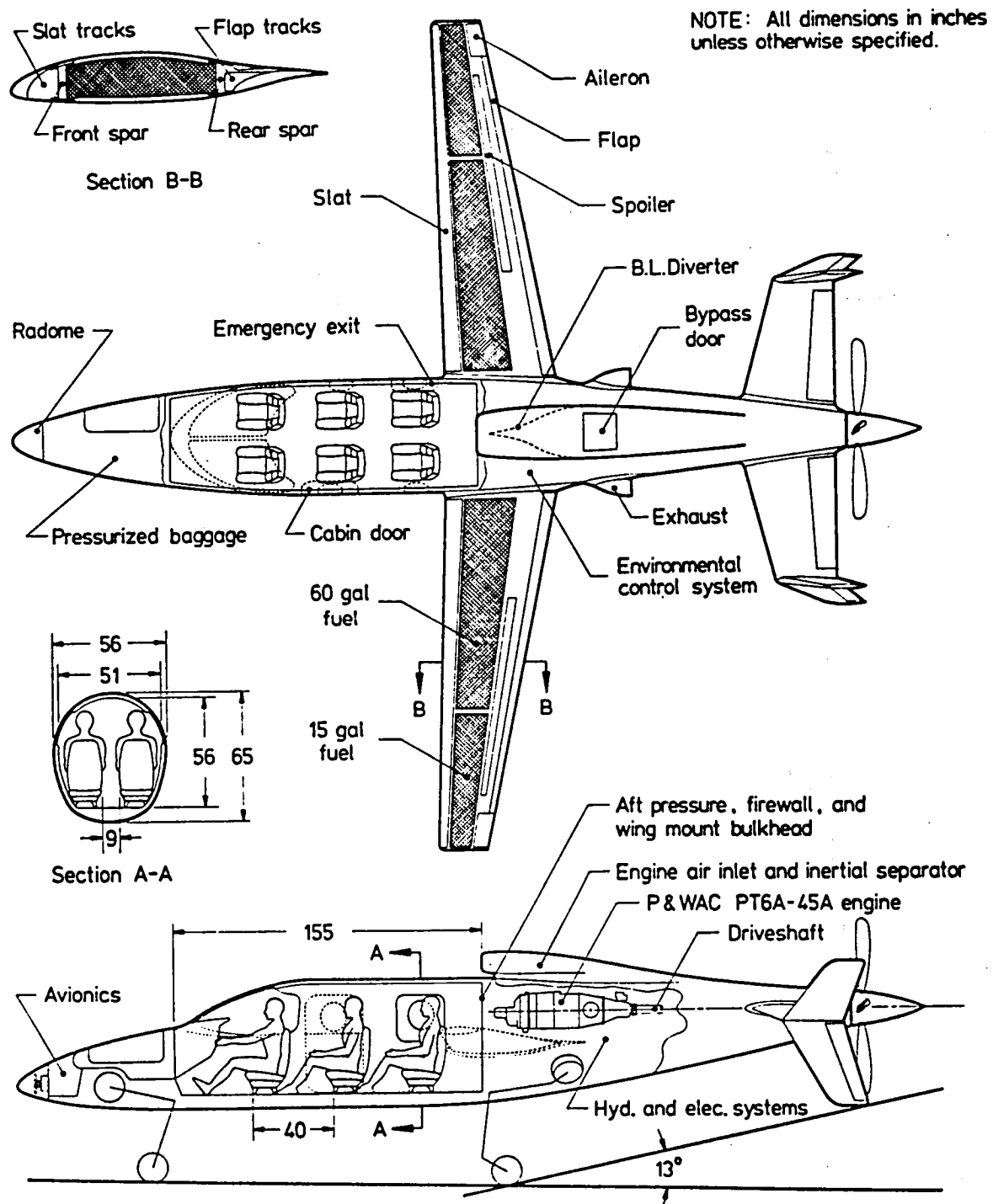
Figure 7. - GATP-2A interior arrangement.

slat

wing

forward-facing steps
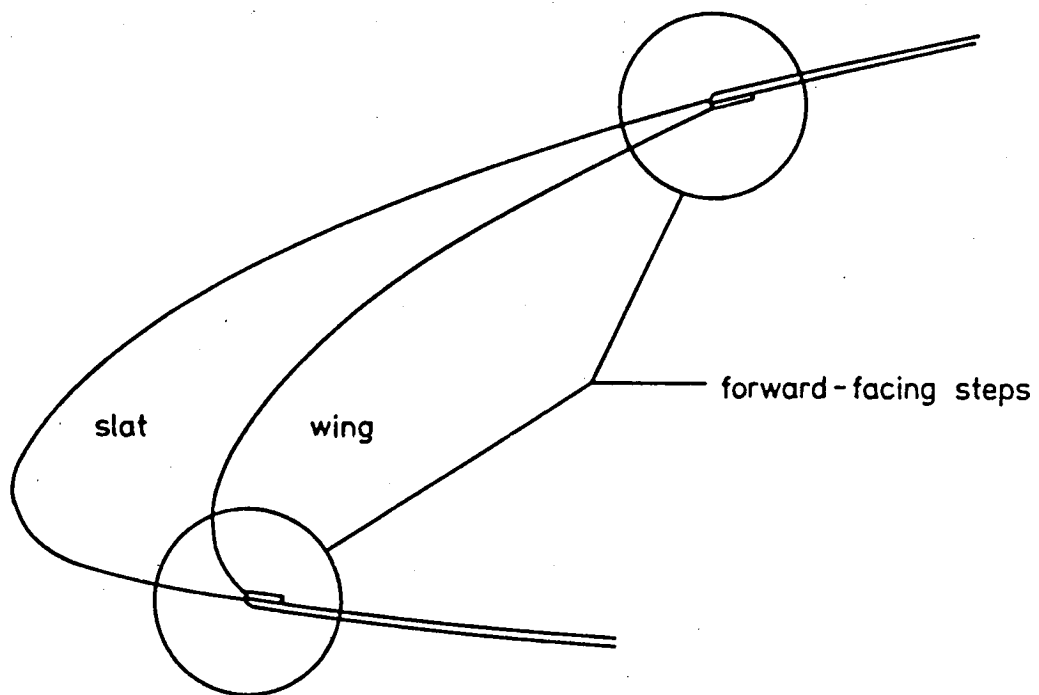
Figure 8. - Forward-facing step concept for leading-edge device integration (step height exaggerated for clarity).
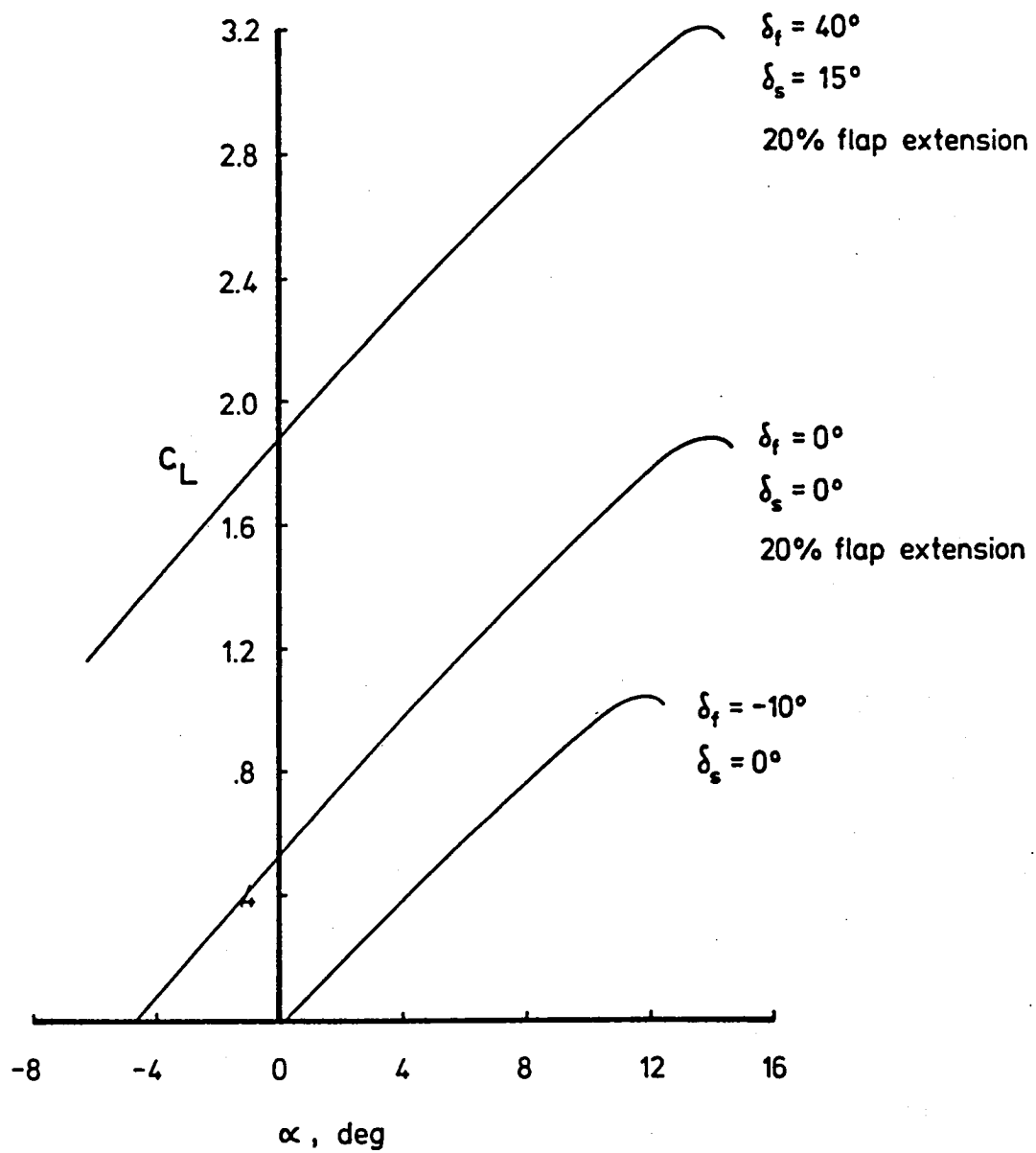
Figure 9. - Untrimmed lift curves for various deflections of the high-lift system.
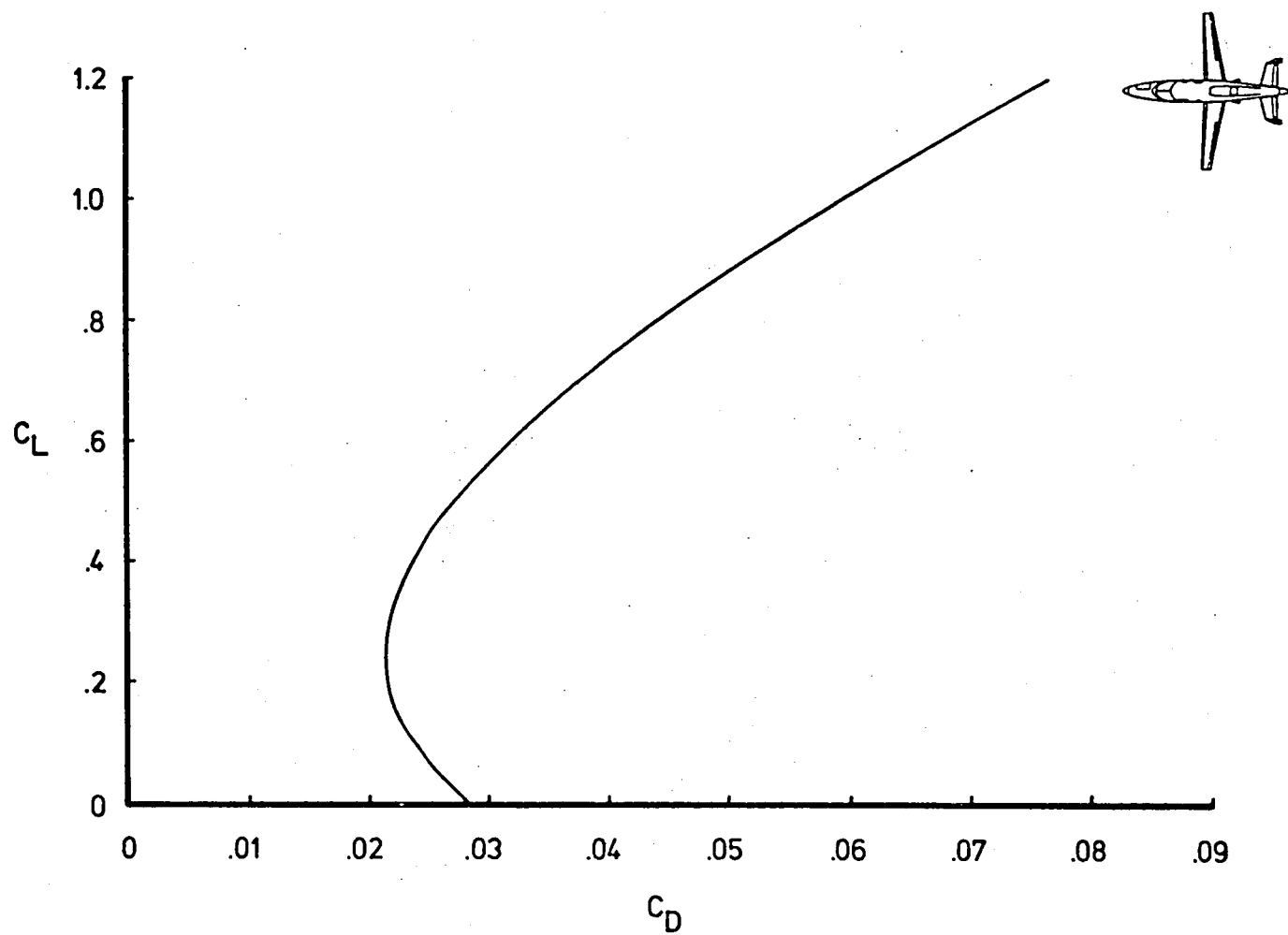
Figure 10. - GATP-2A cruise drag polar.
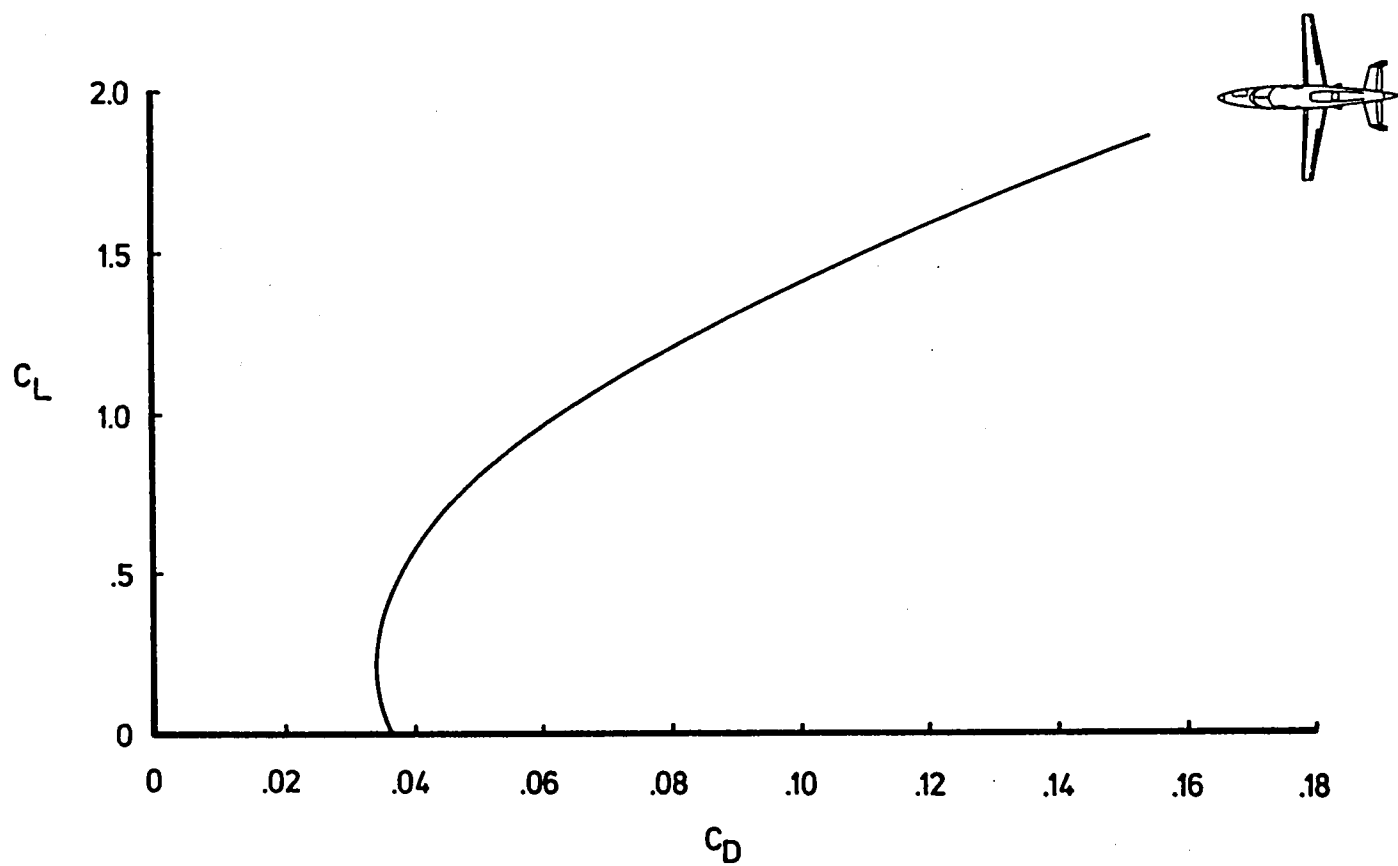
Figure 11. - GATP-2A takeoff drag polar, gear drag not included.
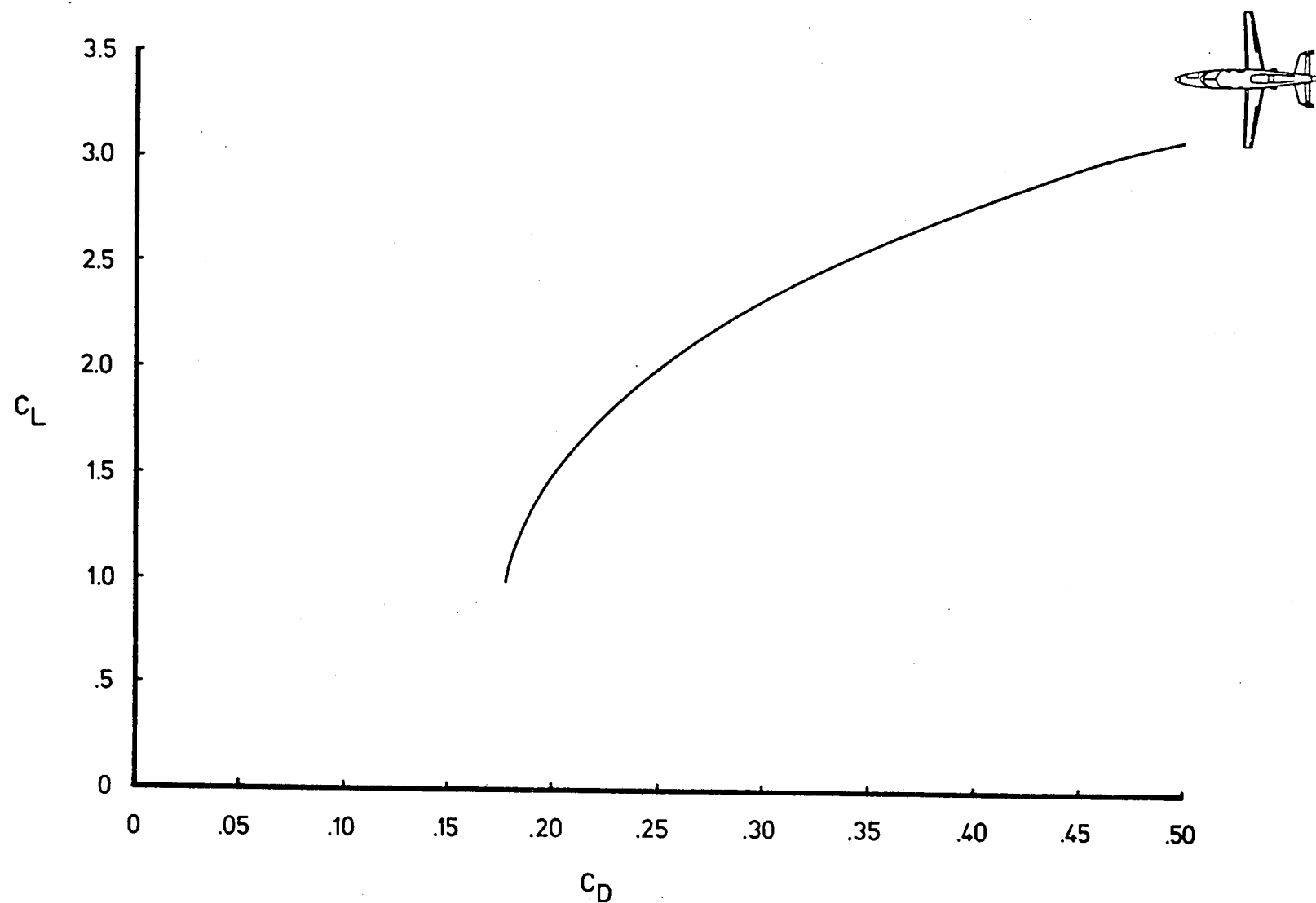
Figure 12. - GATP-2A landing drag polar, gear drag not included.
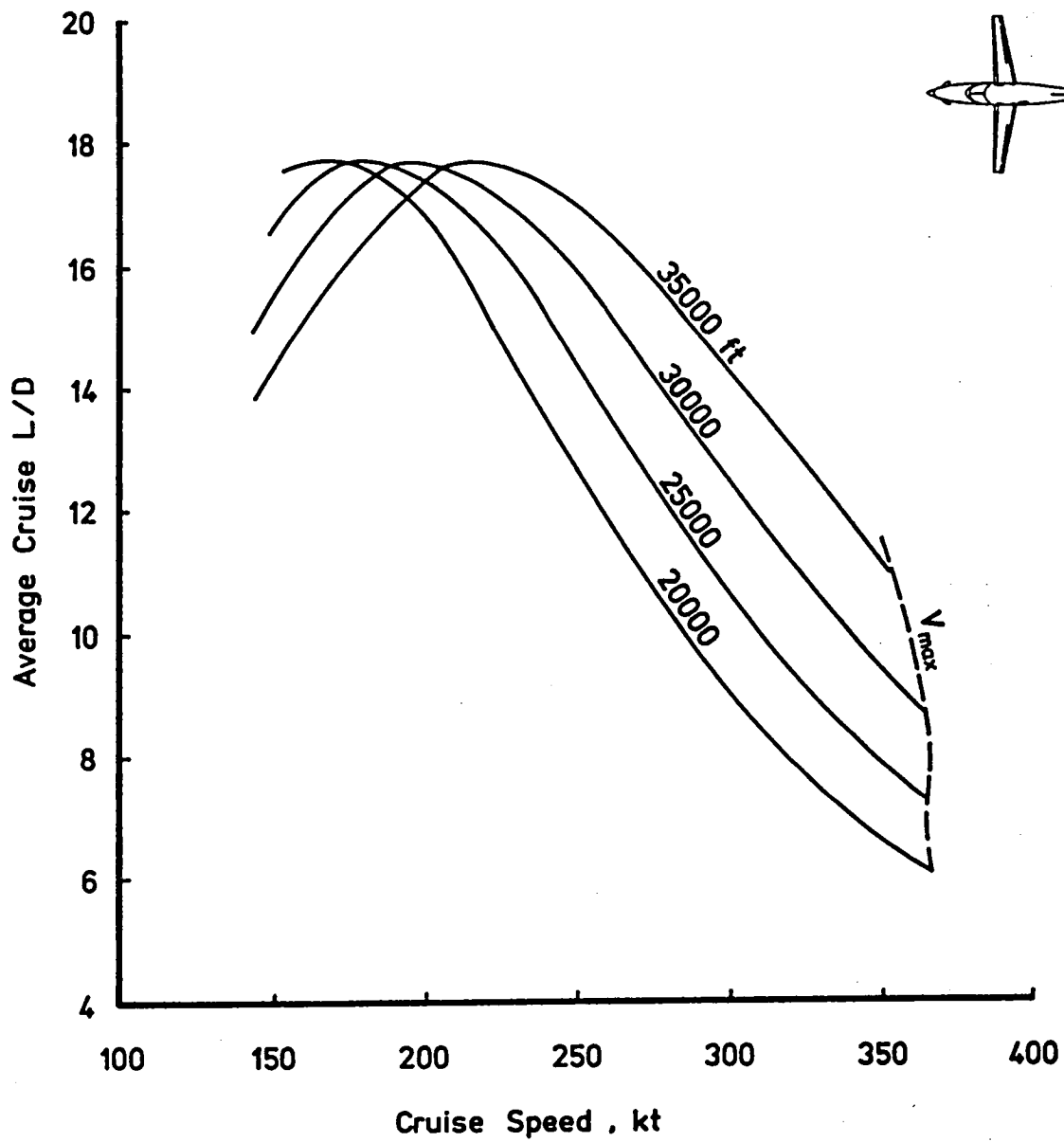
Figure 13. - GATP-1B cruise lift-drag ratios.
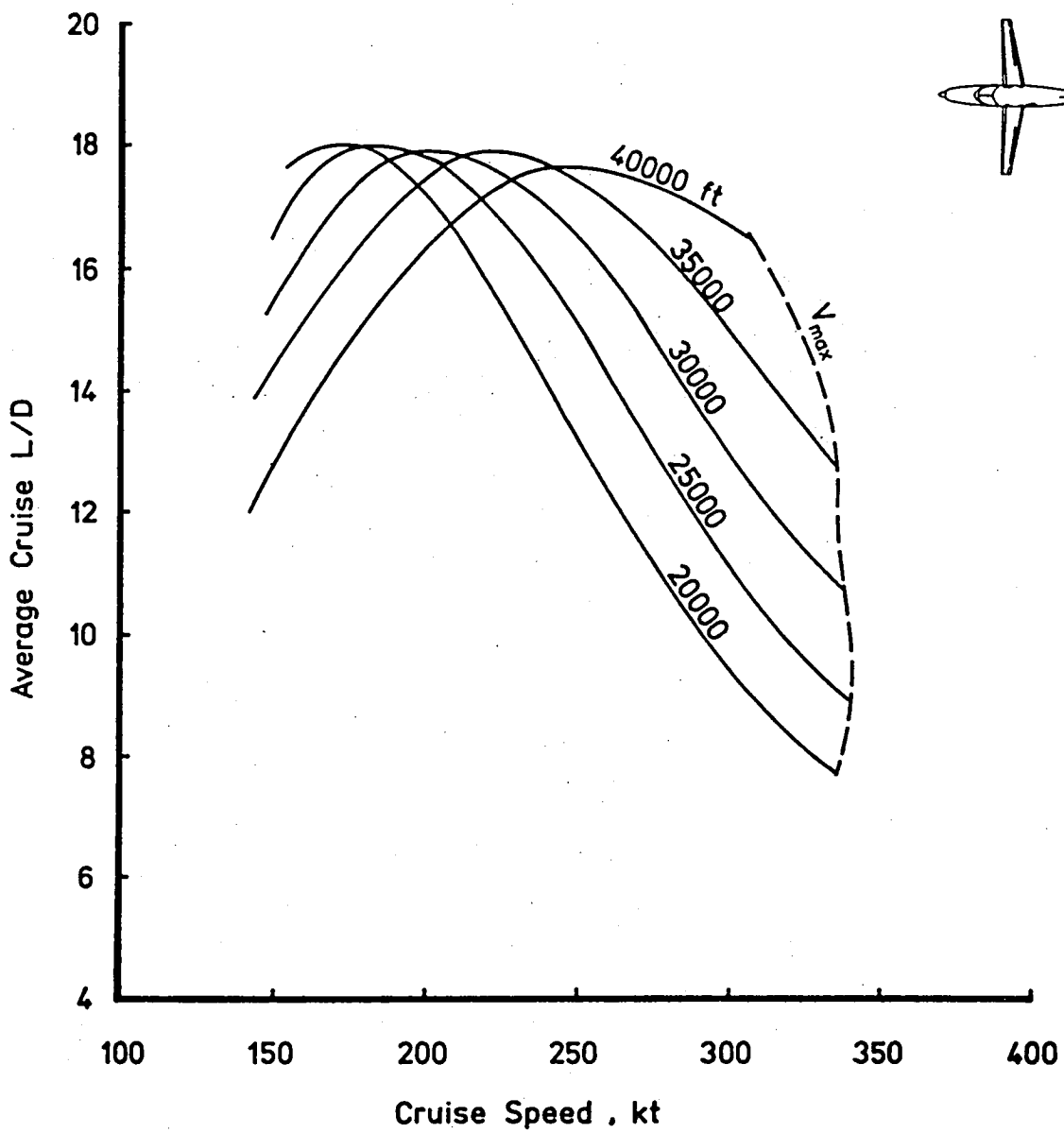
Figure 14. - GATP-1C cruise lift-drag ratios.
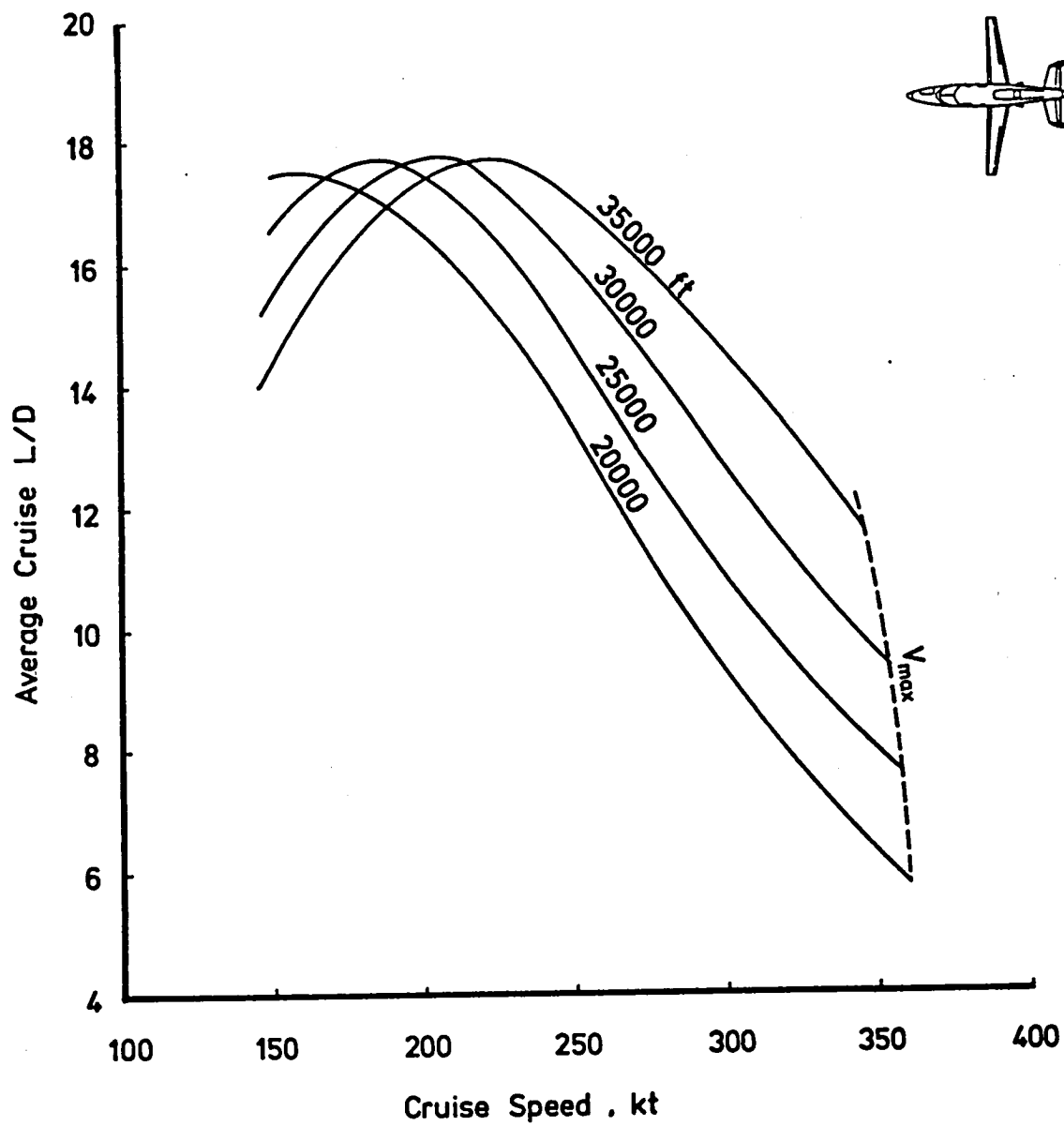
Figure 15. - GATP-2A cruise lift-drag ratios.
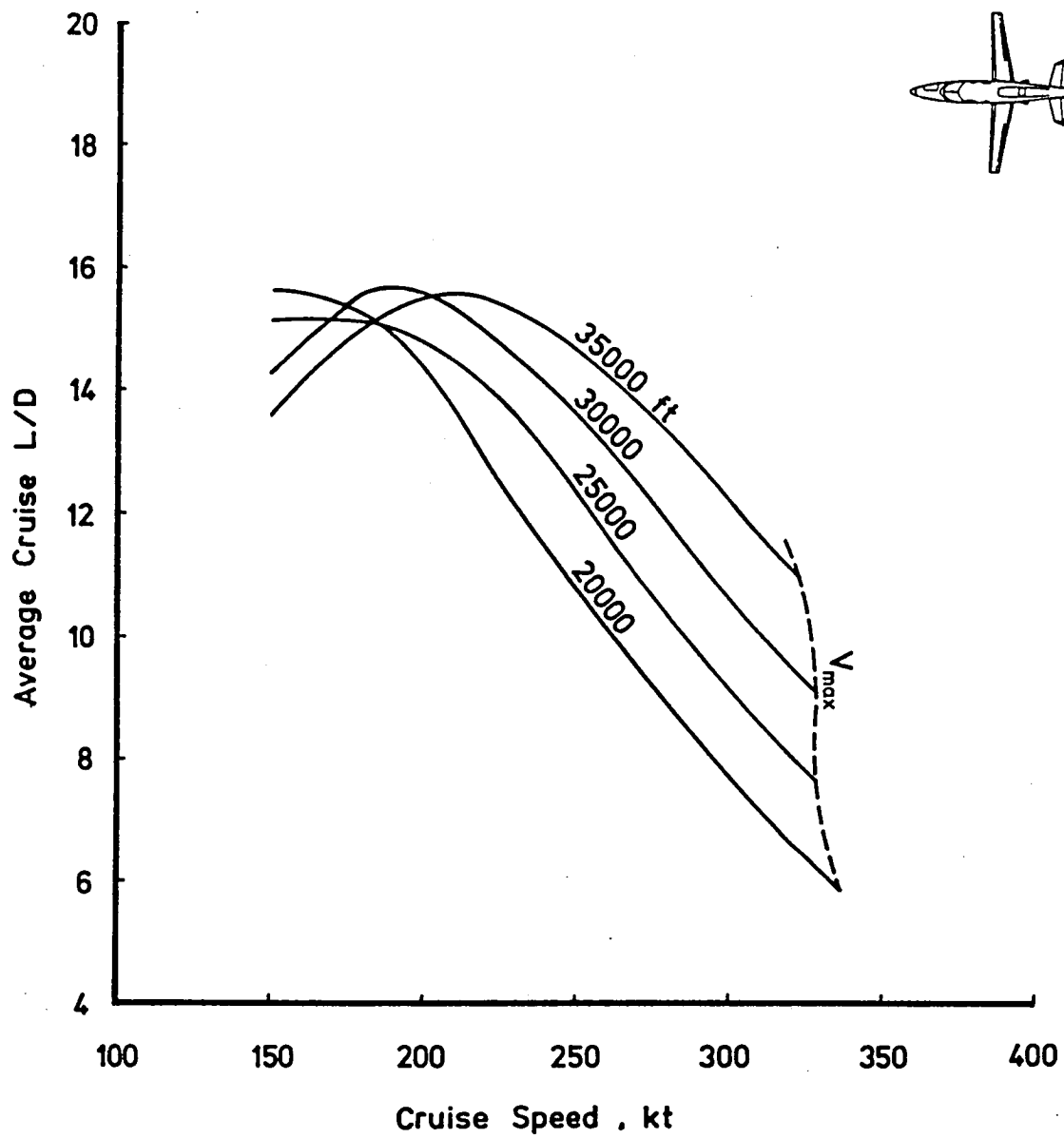
Figure 16. - GATP-2C cruise lift-drag ratios.
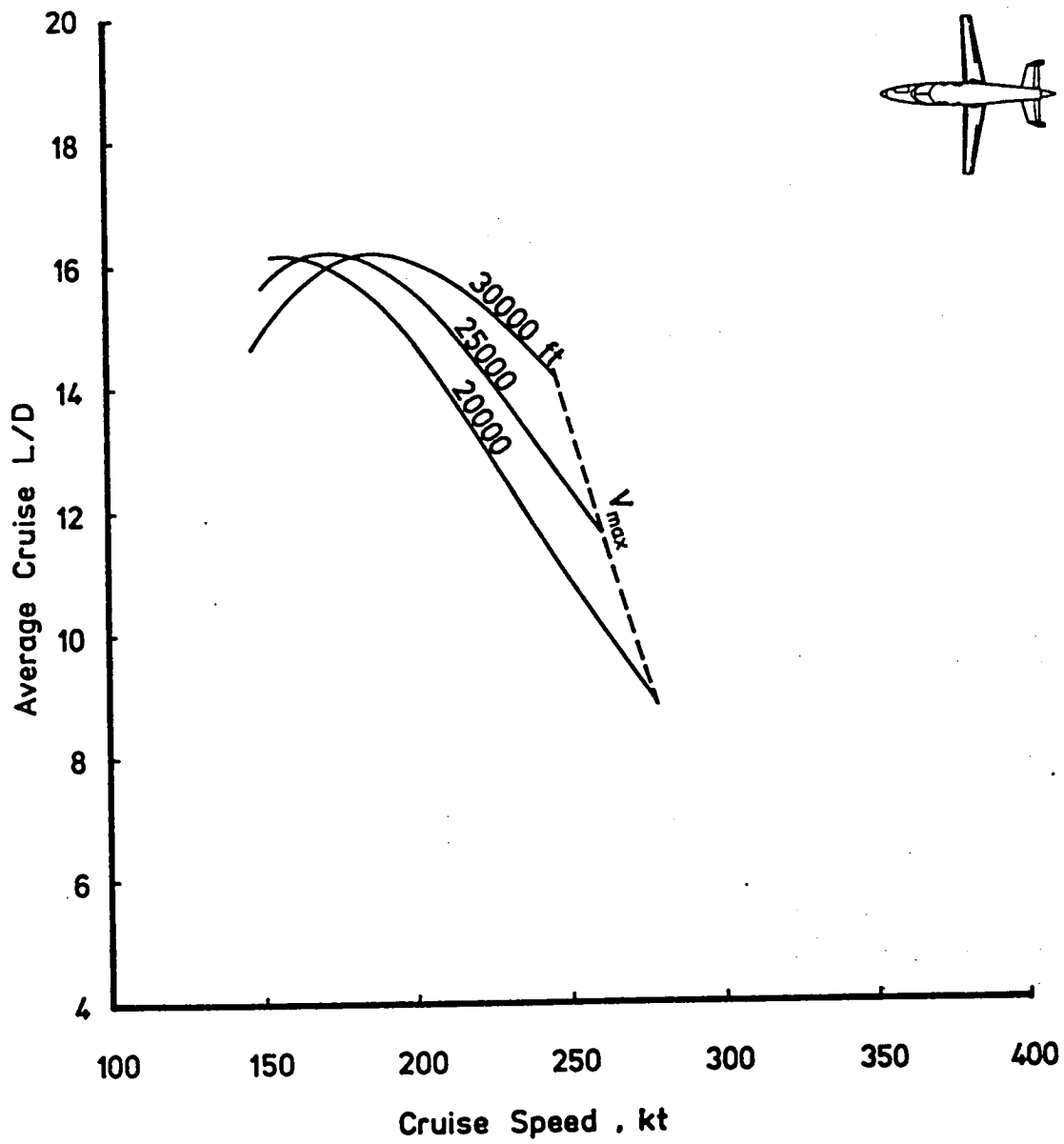
Figure 17. - GATP-2D cruise lift-drag ratios.
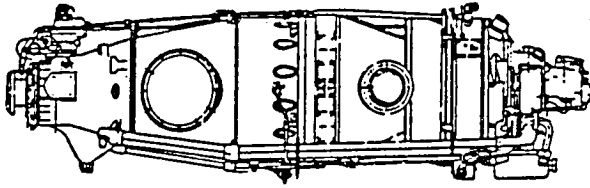
Pratt & Whitney PT6A-45A
overall length = 71.9 in
diameter = 22.5 in
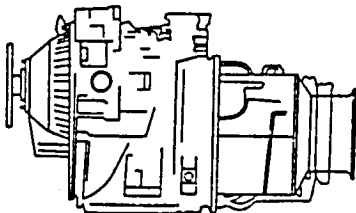
Garrett TPE 331-11
overall length = 43.4 in
overall width = 21.7 in
overall height = 27.2 in
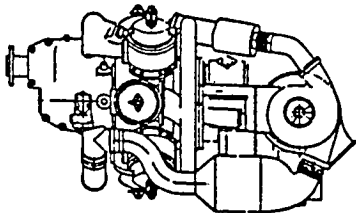
Teledyne Continental diesel
overall length = 43.3 in
overall width = 29.5 in
overall height = 27.5 in

Figure 18. - Study engine geometry comparison.

58
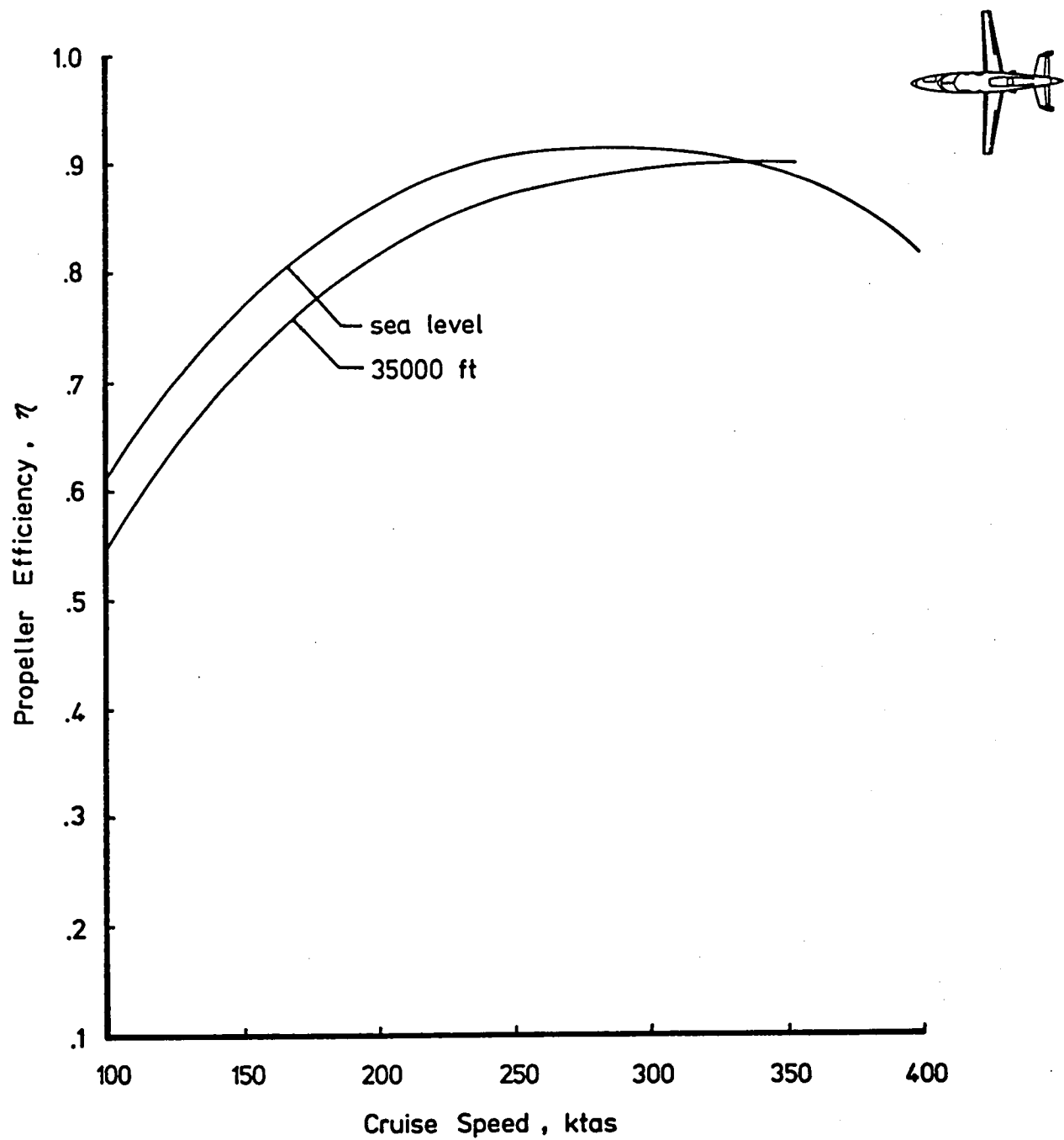
Figure 19. - GATP-2A propeller efficiency variation, maximum cruise power.
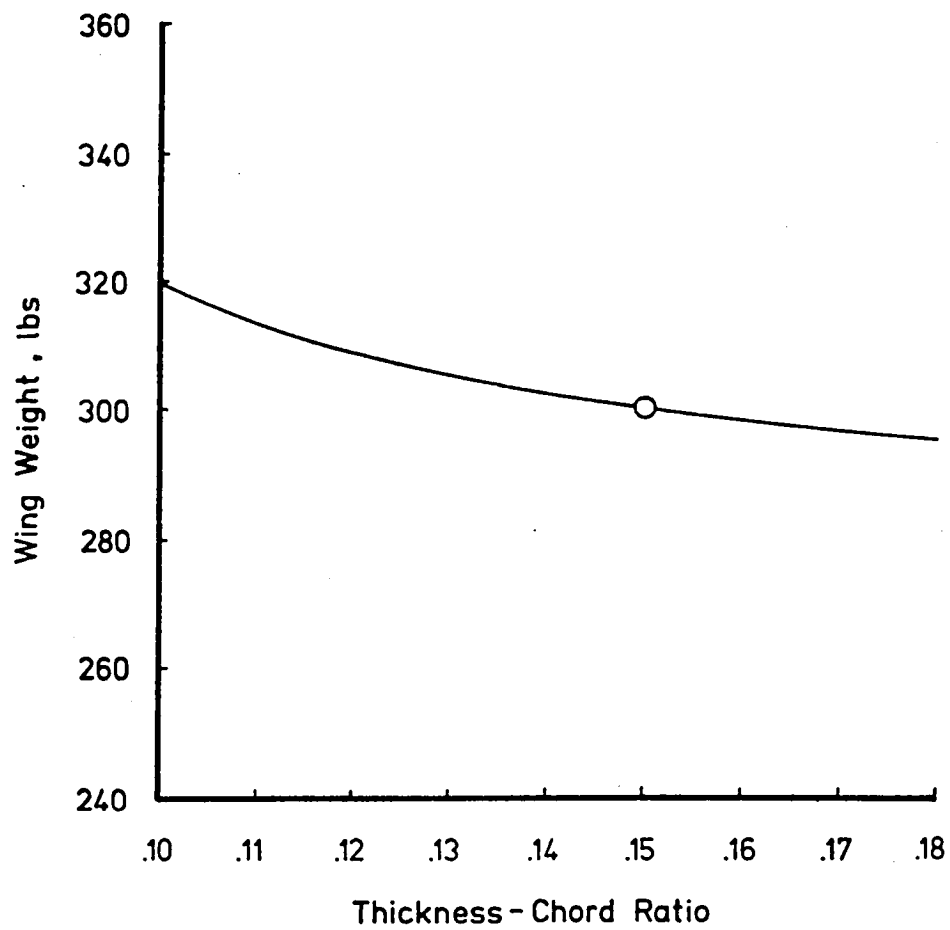
Figure 20. - GATP-2A wing weight variation with thickness ratio.
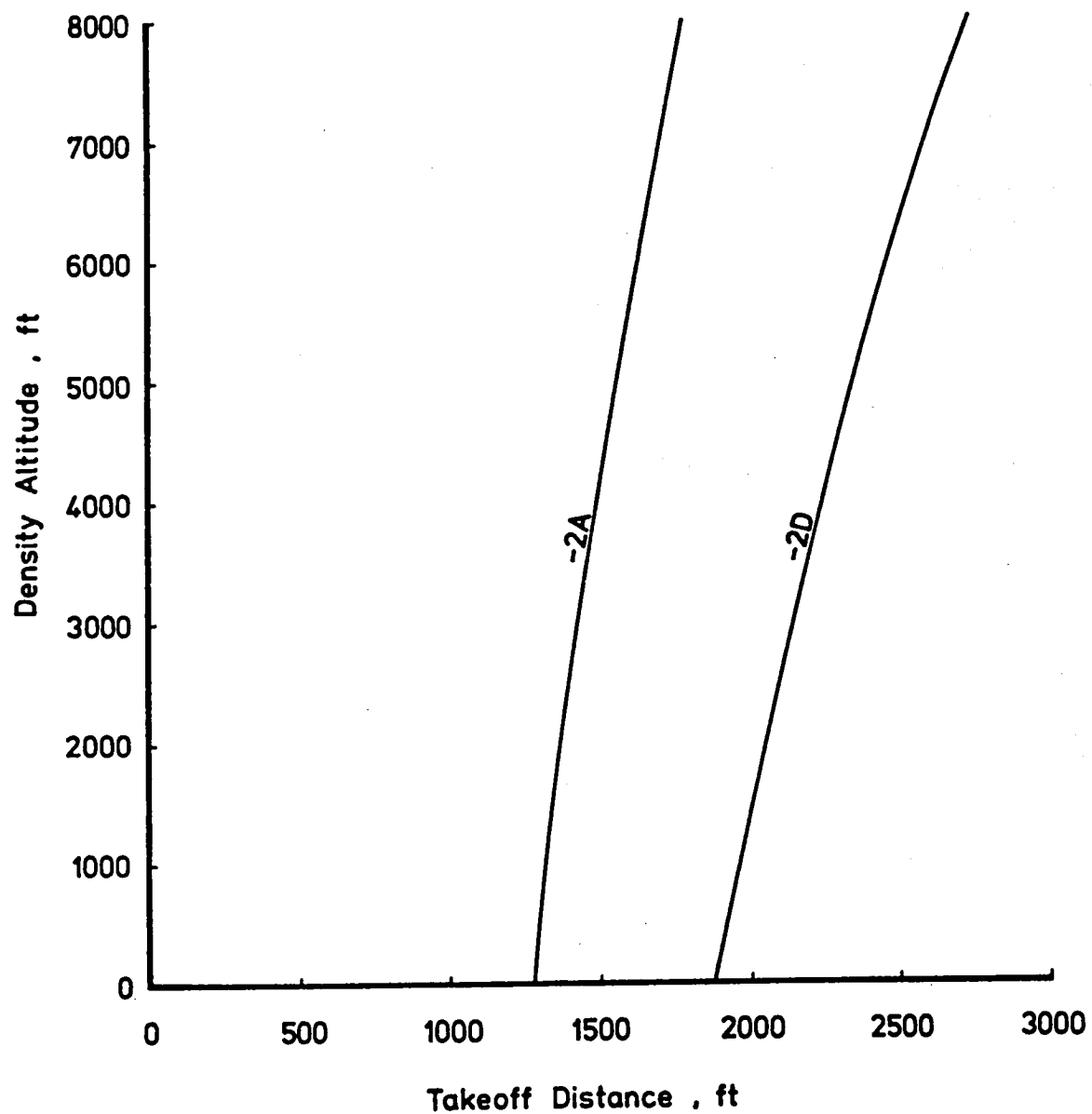
Figure 21. - Comparison of study aircraft takeoff distances over a 50 ft obstacle, maximum TOGW.
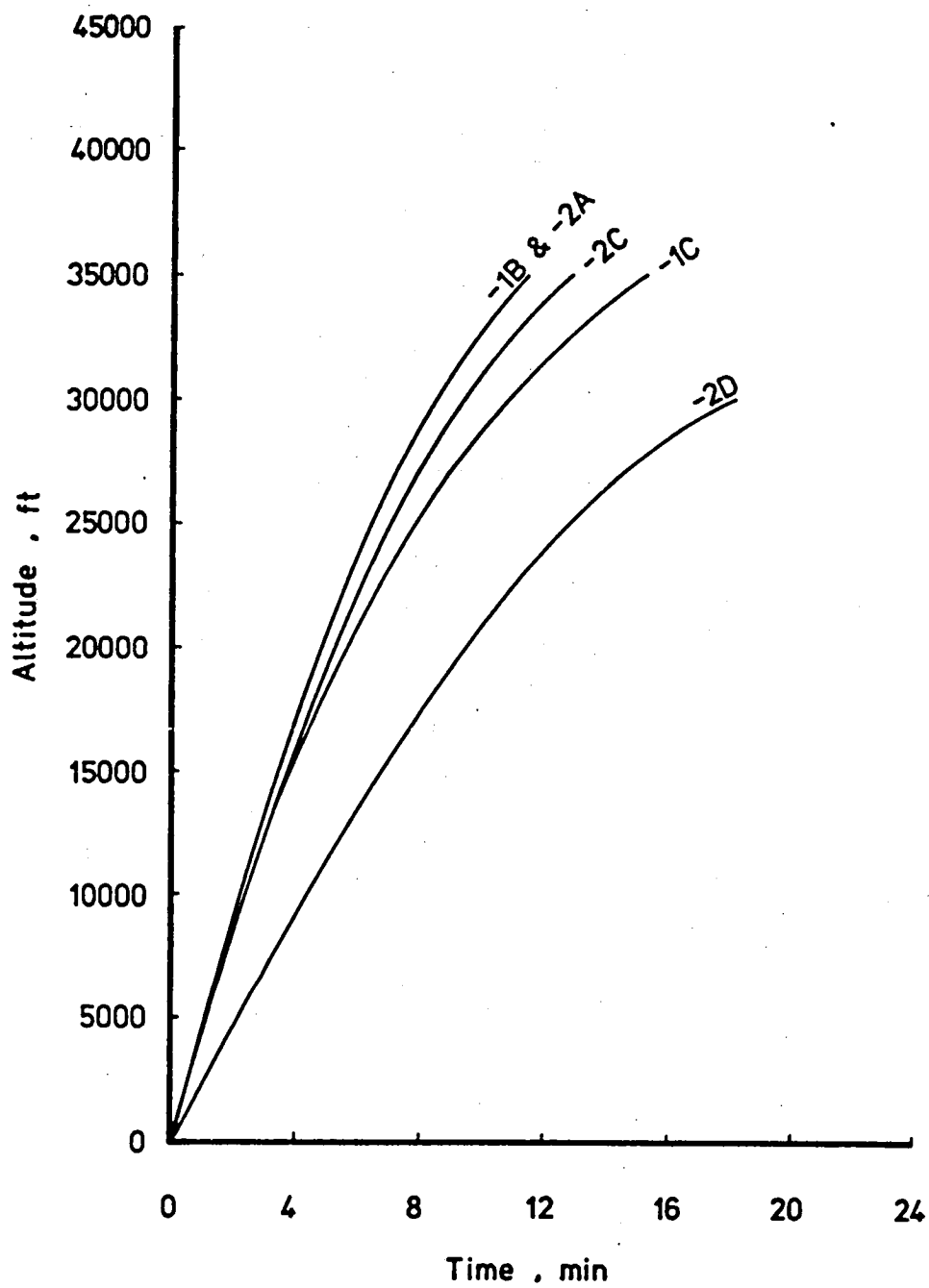
Figure 22. - Comparison of study aircraft time to climb, maximum TOGW.
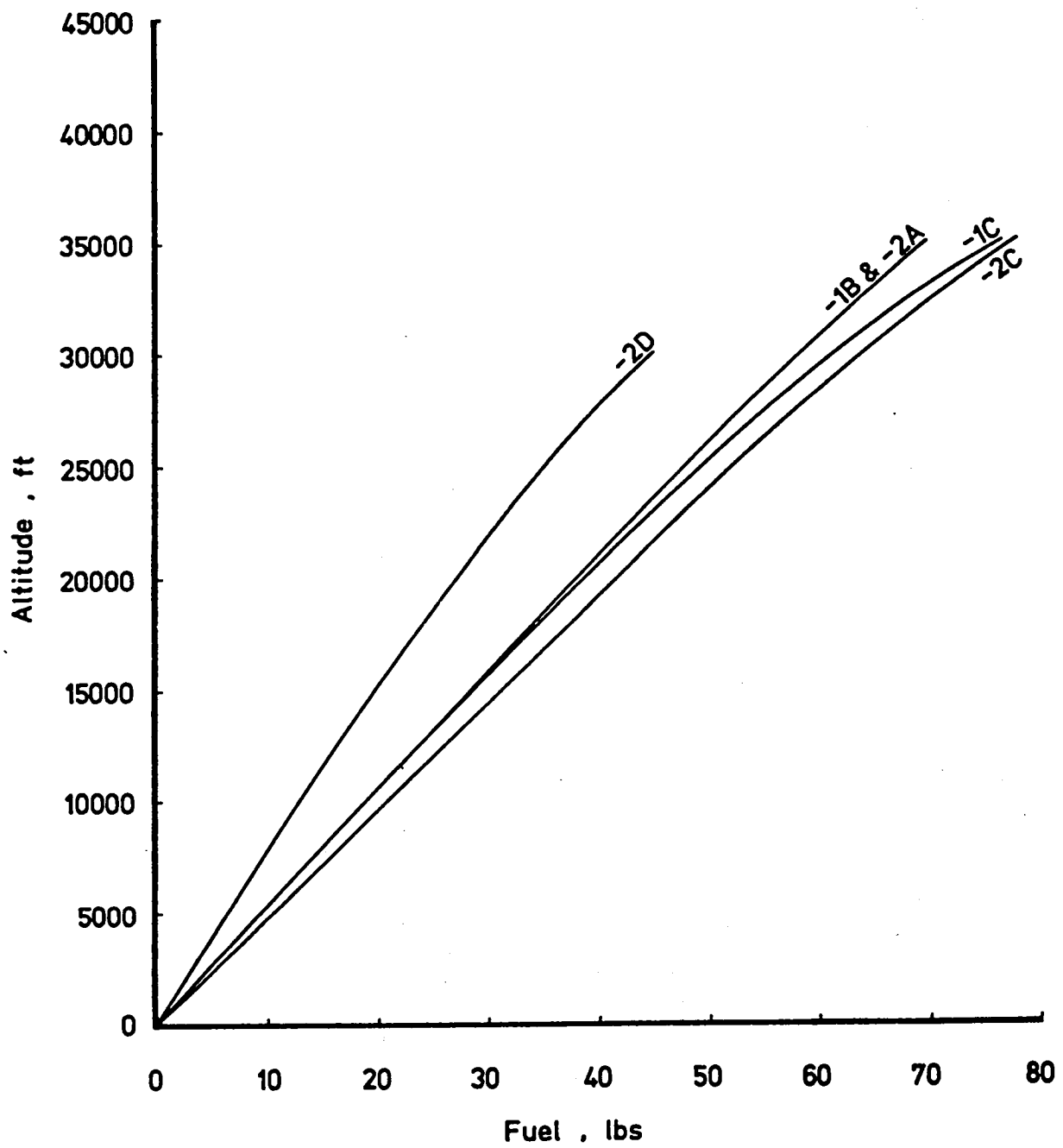
Figure 23. - Comparison of study aircraft fuel to climb, maximum TOGW.
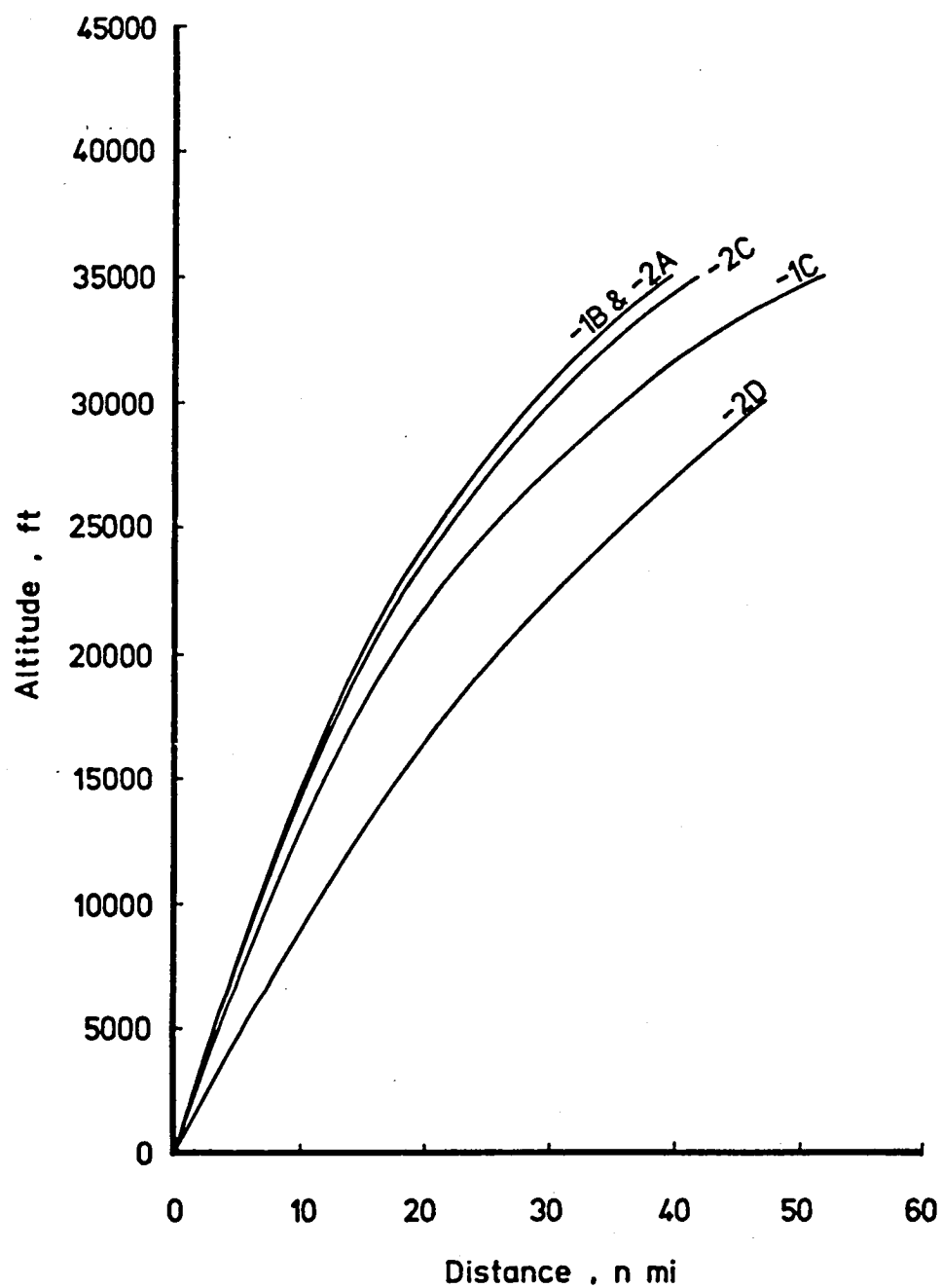
Figure 24. - Comparison of study aircraft distance to climb, maximum TOGW.
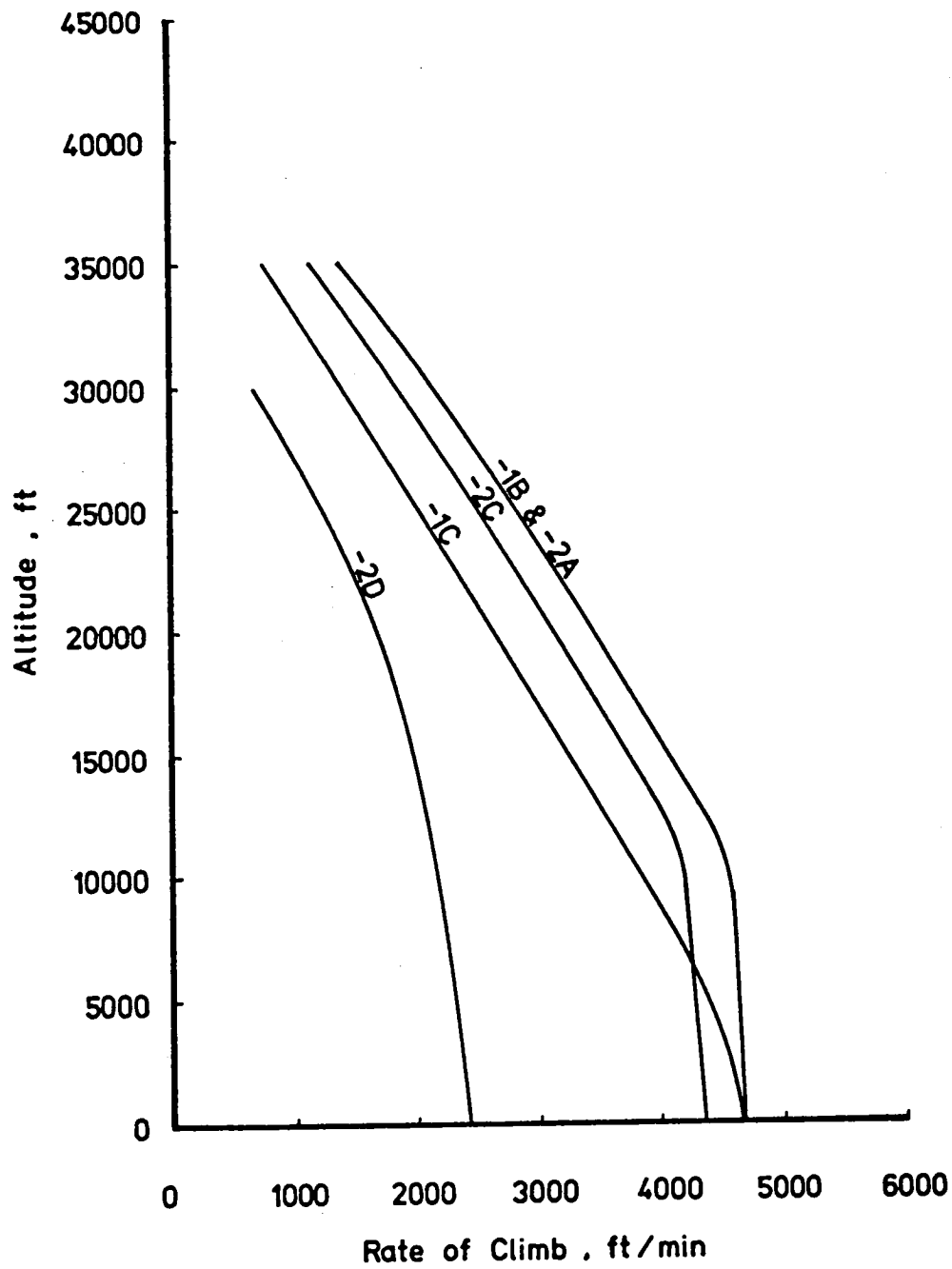
Figure 25. – Comparison of study aircraft rate of climb, maximum TOGW.
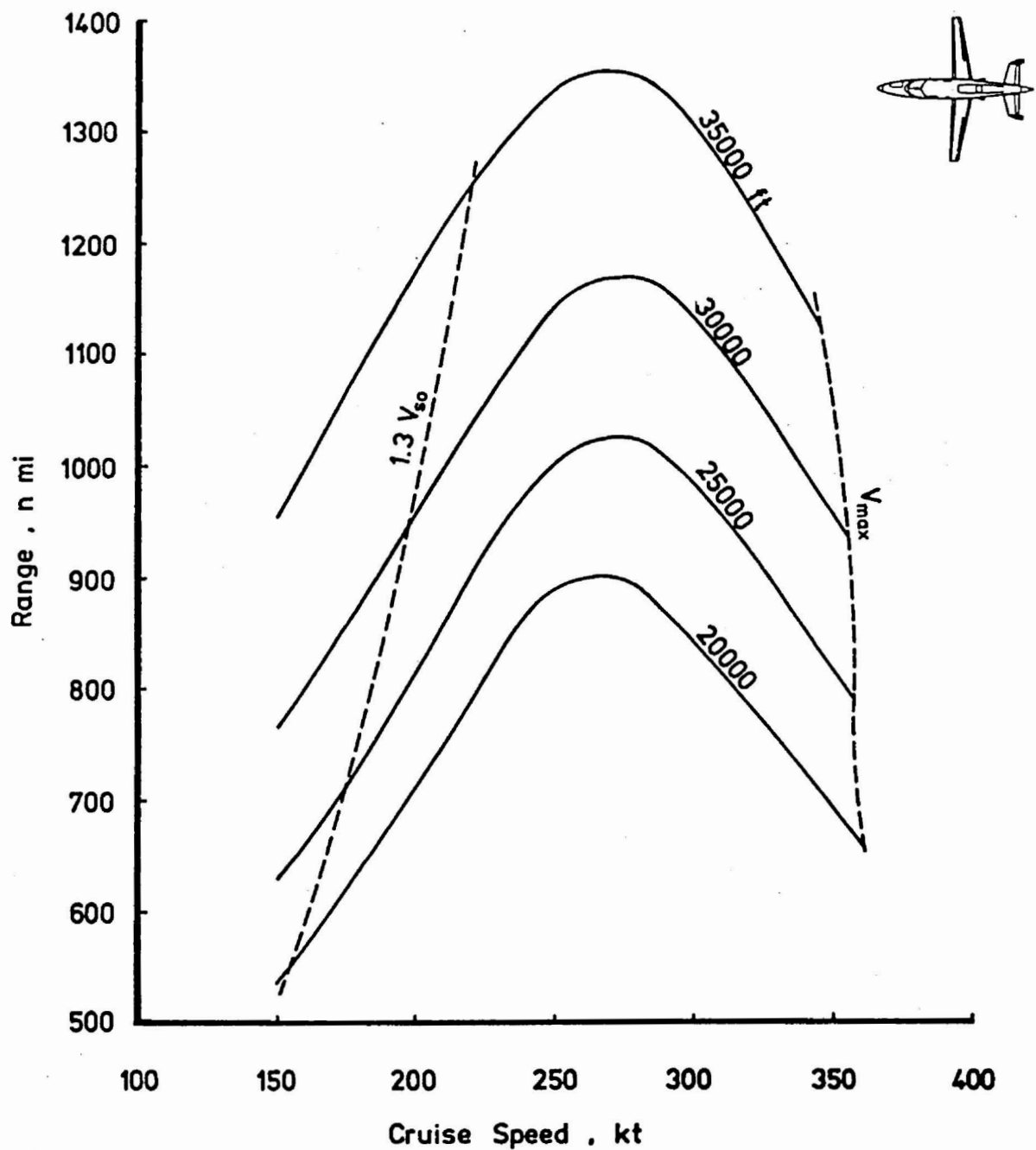
Figure 26. – GATP-2A range for variations in cruise speed and altitude.
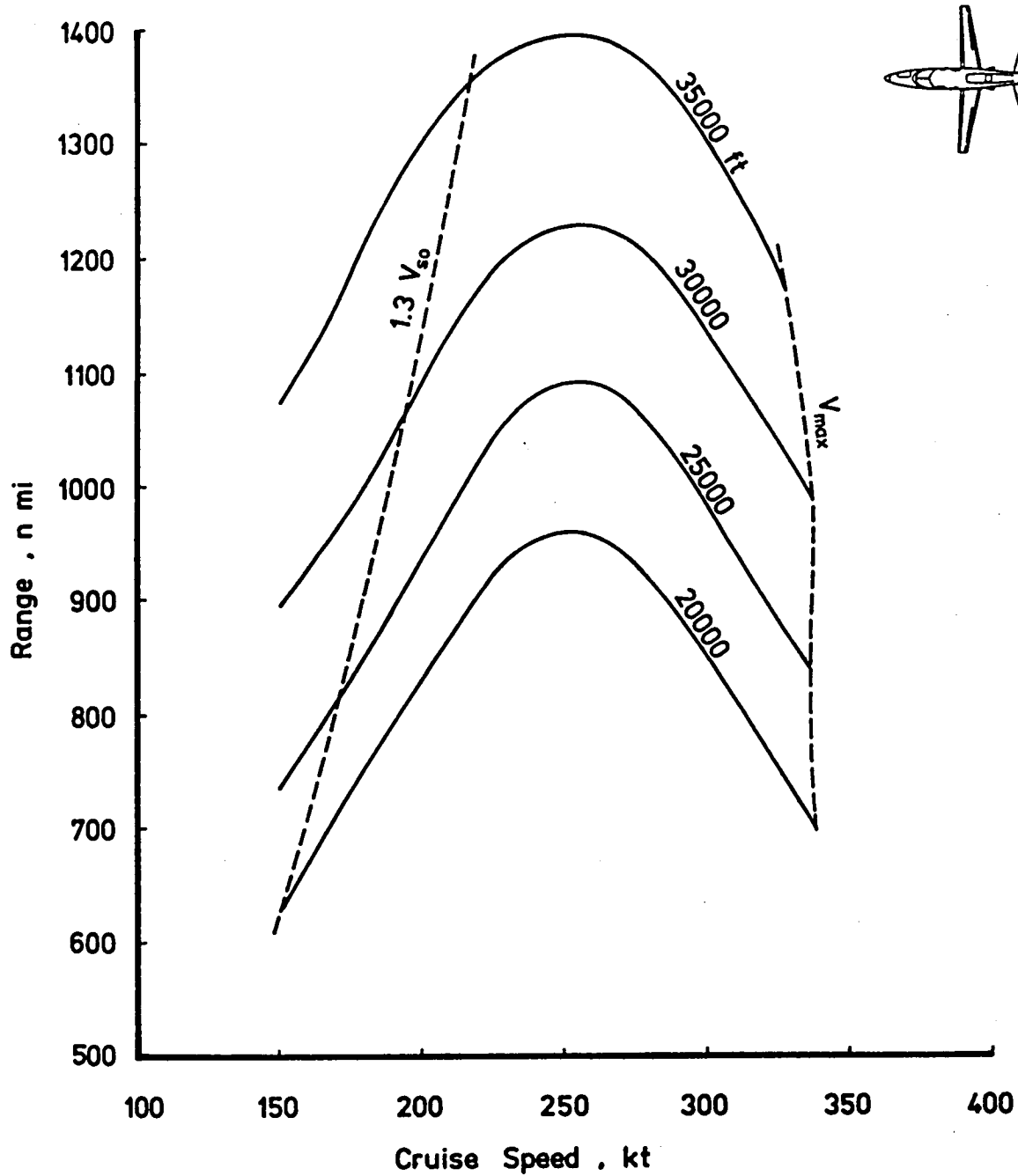
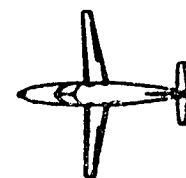Figure 27. - GATP-2C range for variations in cruise speed and altitude.
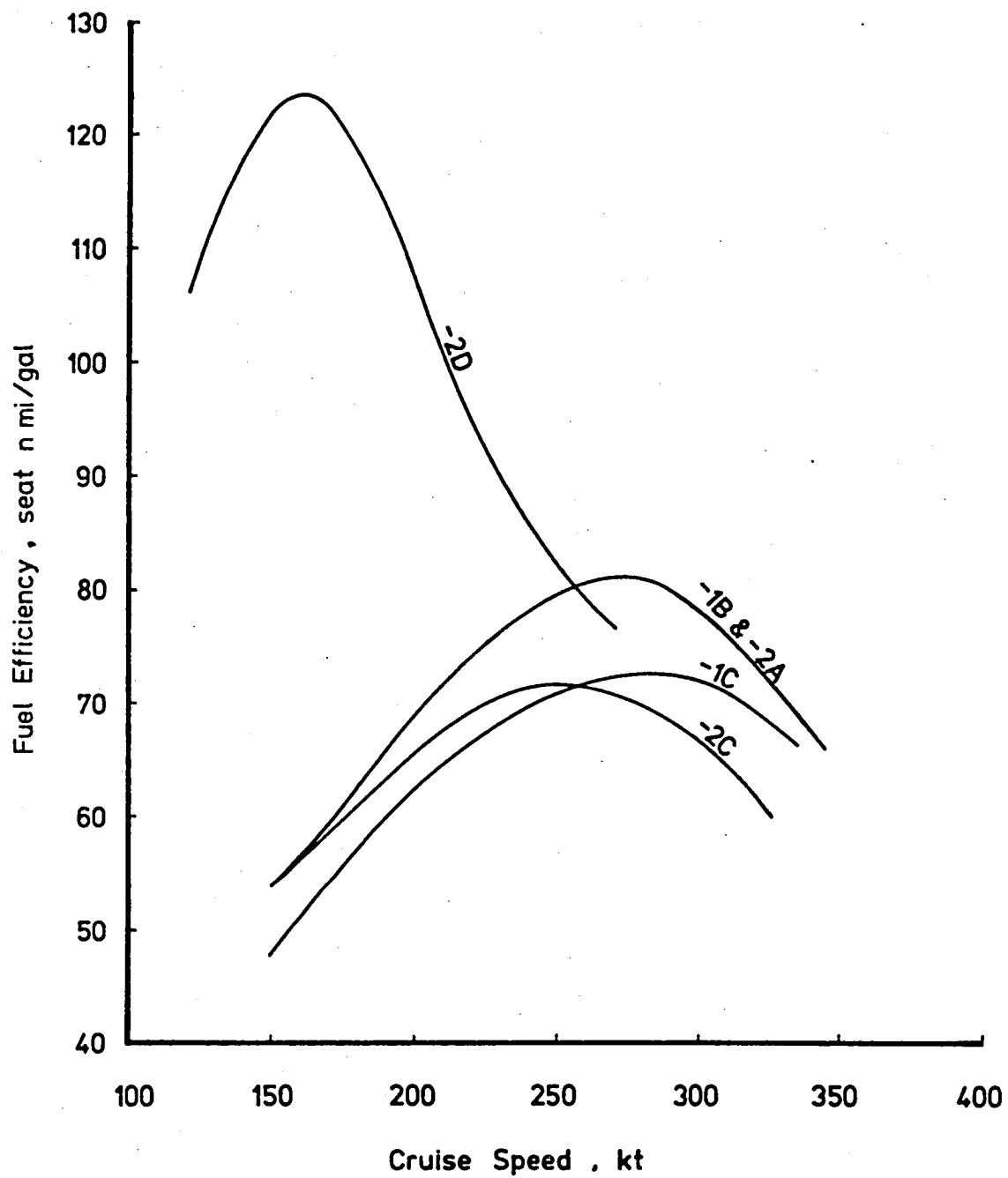
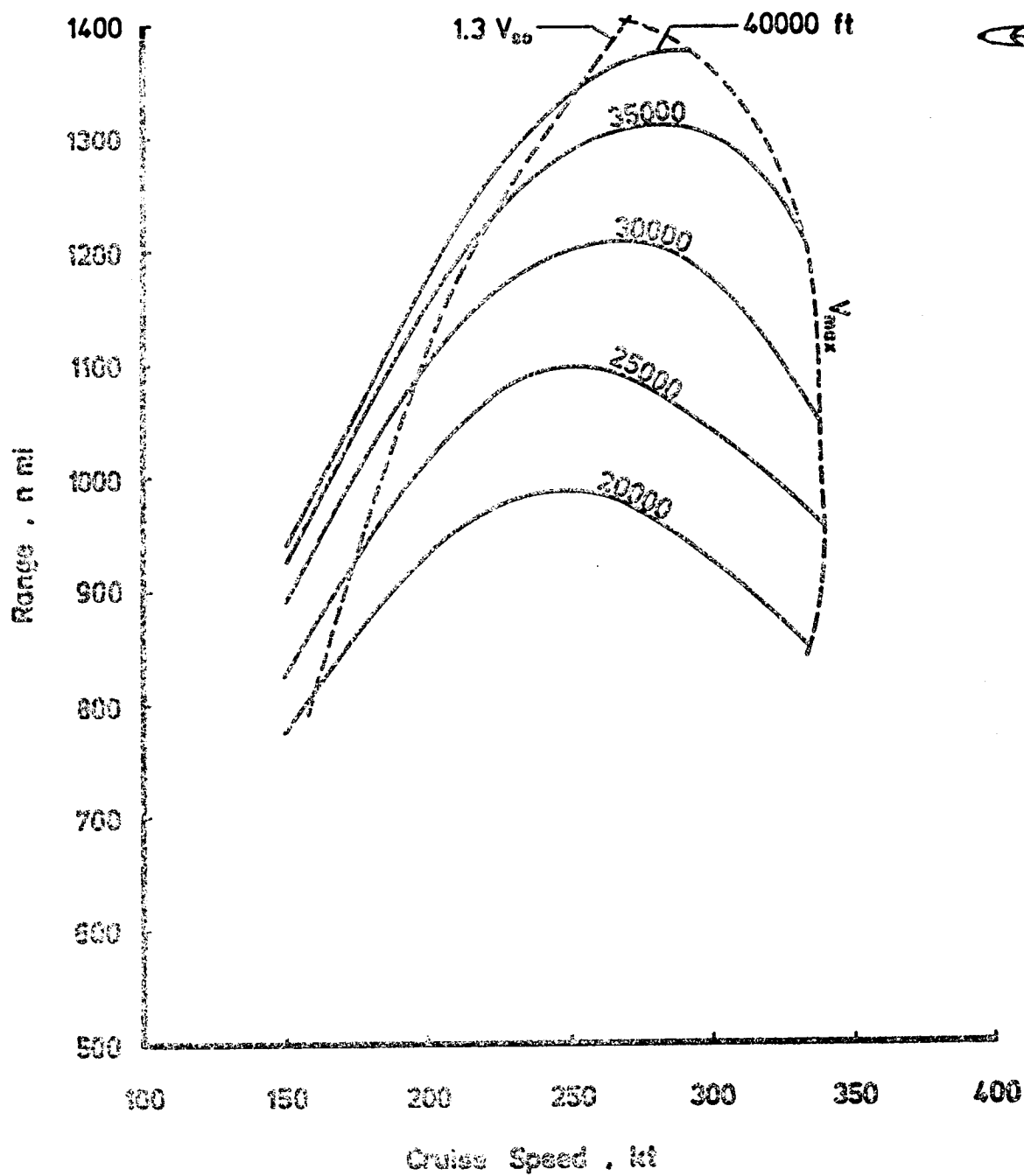Figure 28. - Comparison of study aircraft fuel efficiency, maximum TOGW.
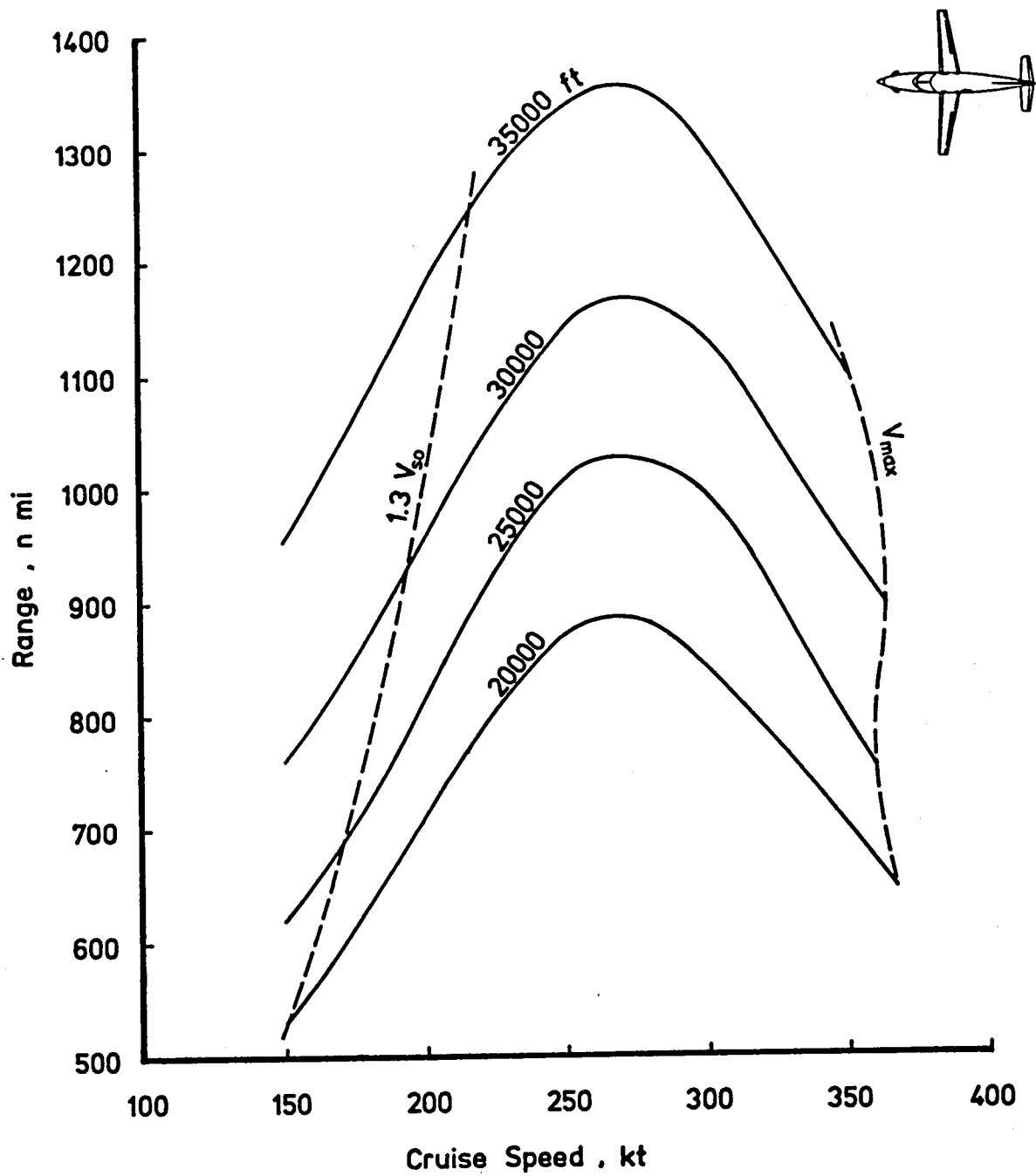
Figure 29. - GATP-1B range for variations in cruise speed and altitude.
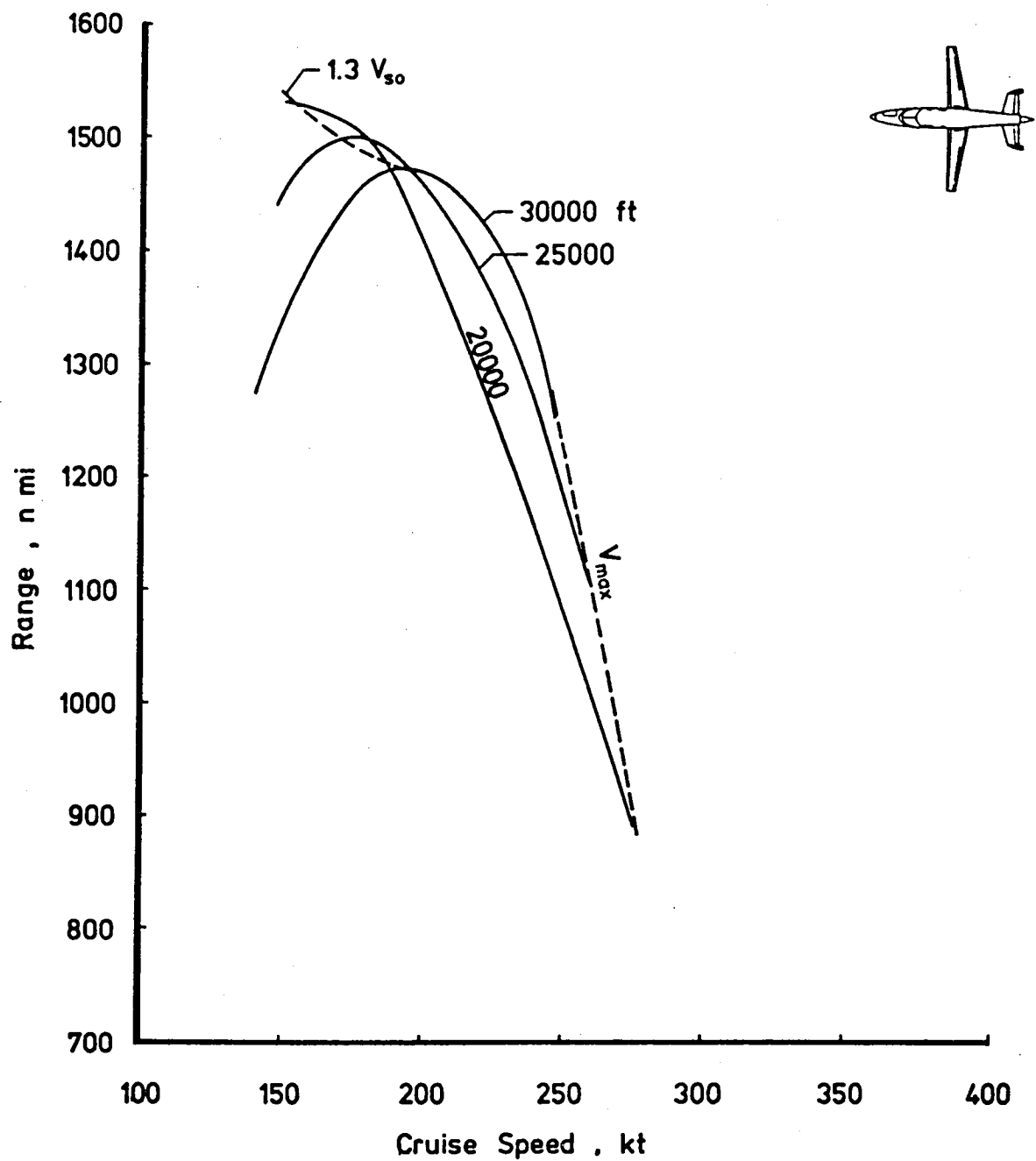
Figure 30. - GATP-2D range for variations in cruise speed and altitude.

Figure 31. - GATP-1C range for variations in cruise speed and altitude.

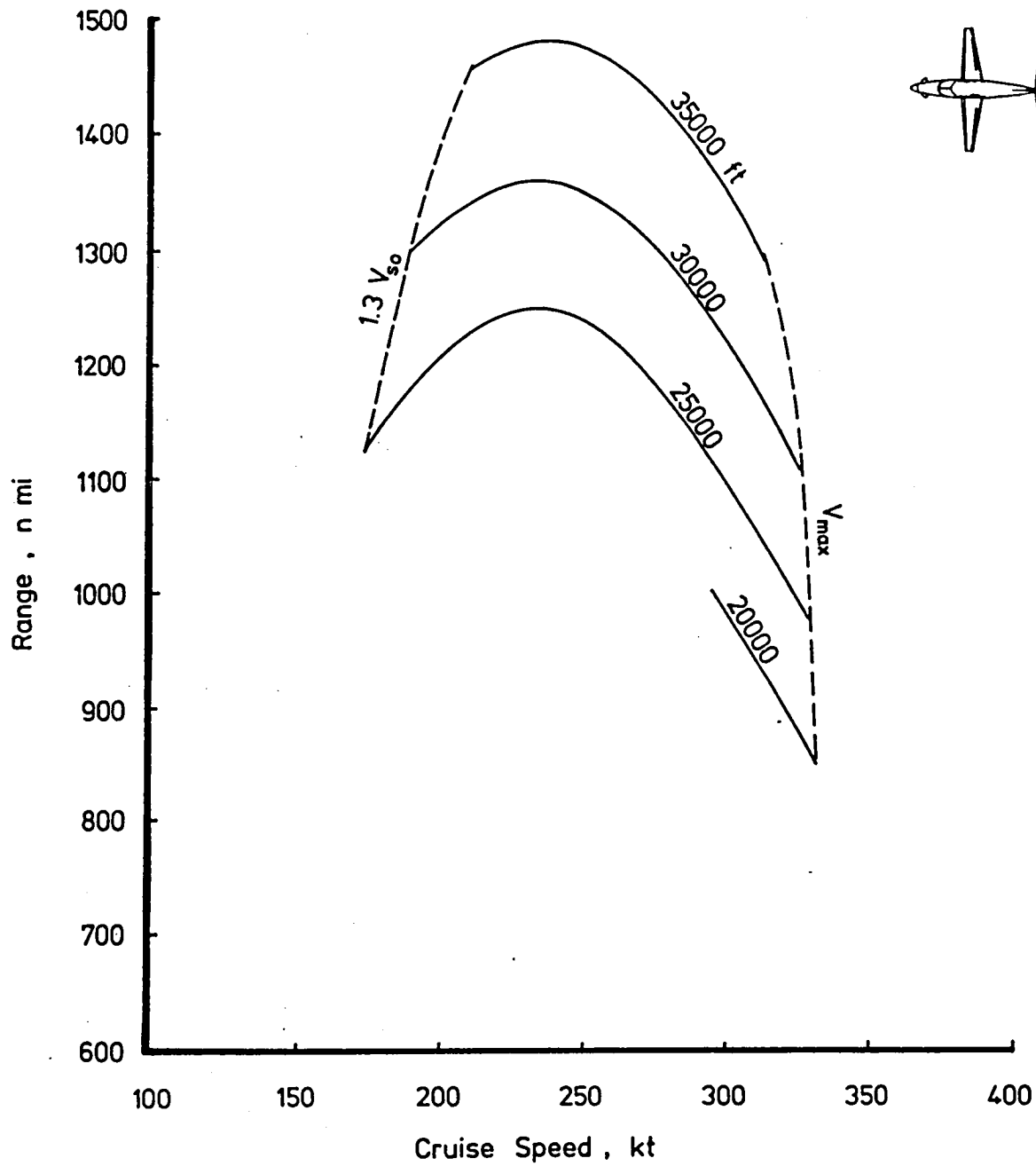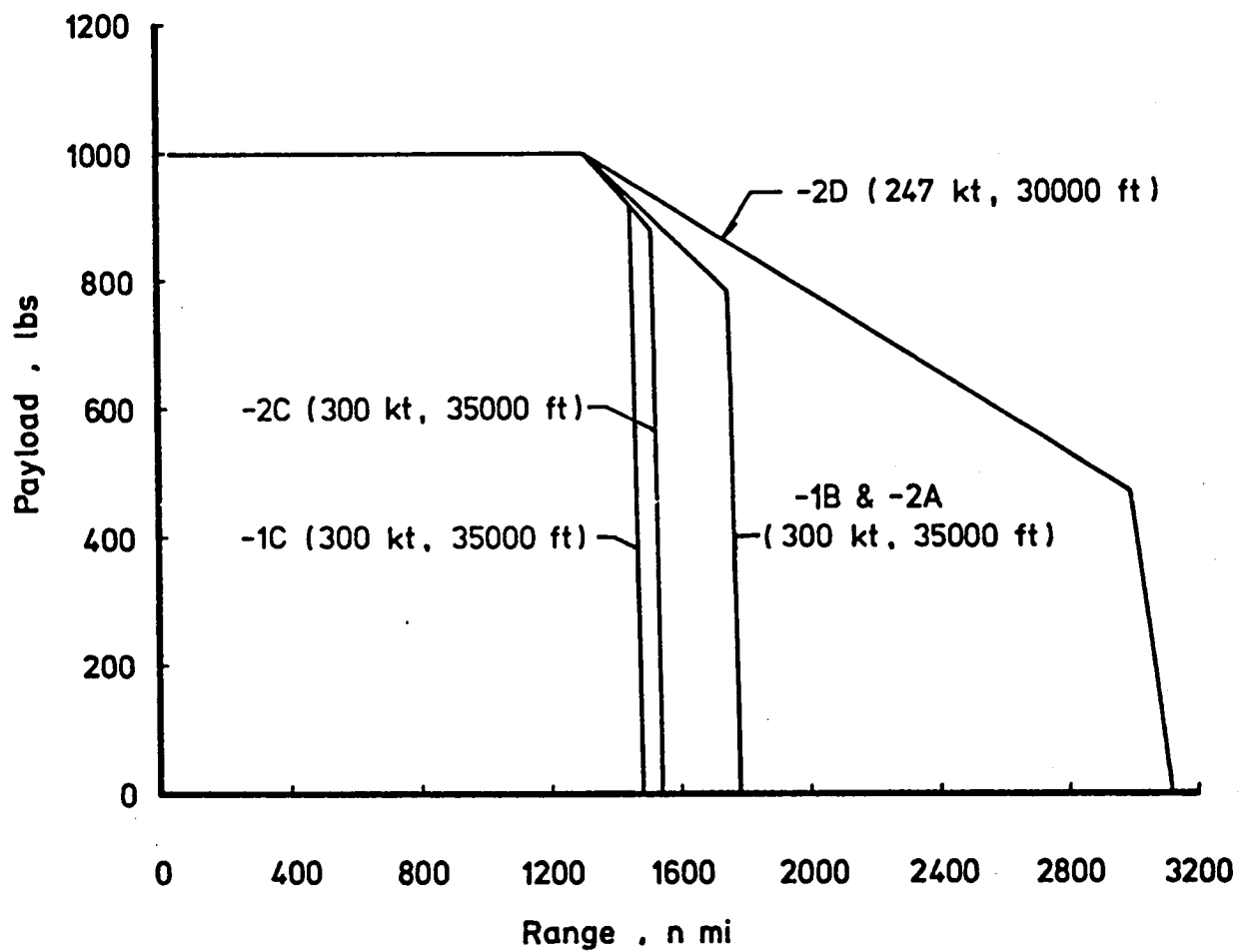Figure 32. - GATP-1A range for variations in cruise speed and altitude. Data from reference 1.

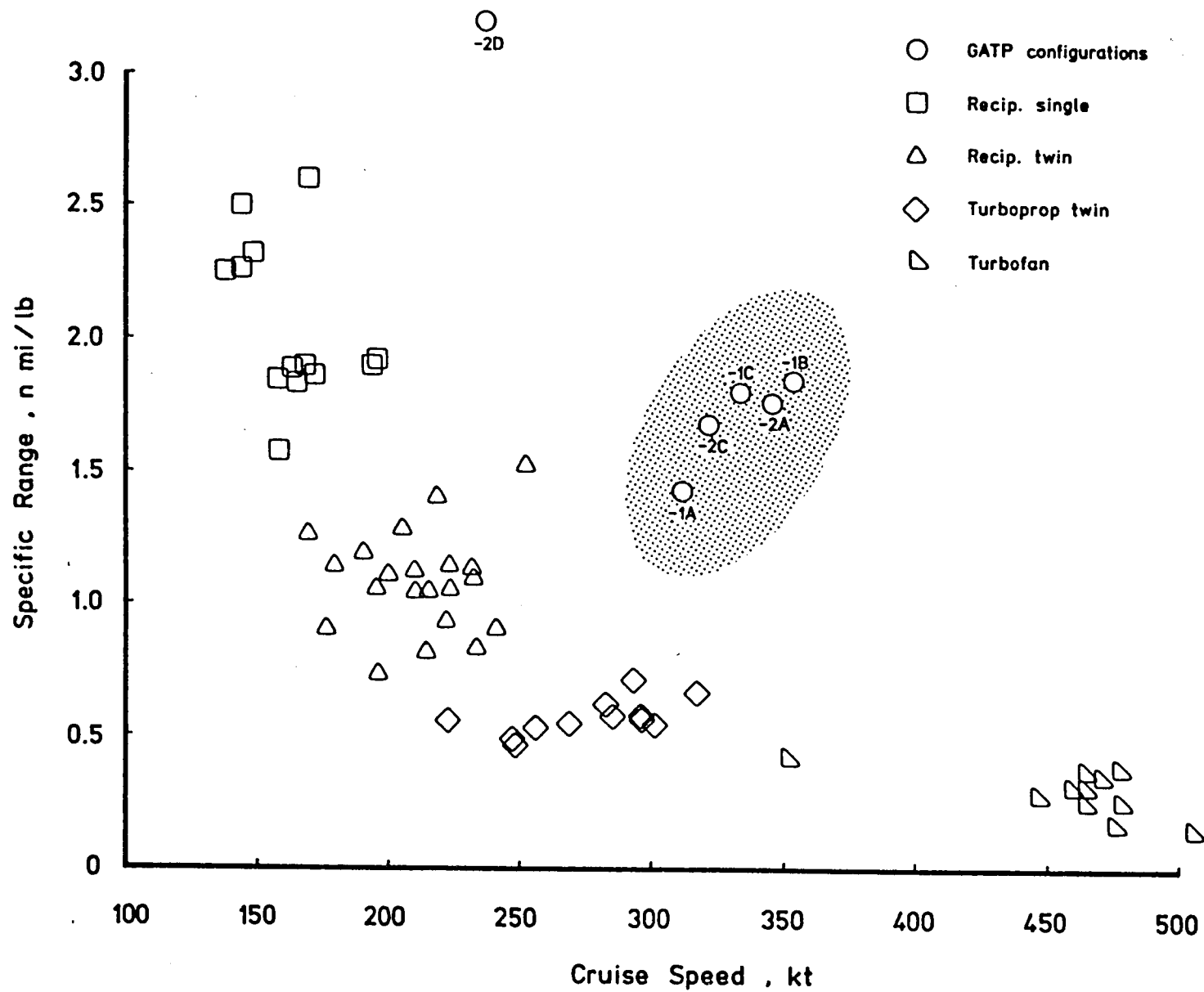Figure 33. – Comparison of study aircraft range-payload capability.

Figure 34. - Comparison of study aircraft cruise fuel efficiency with that of current general aviation airplanes.
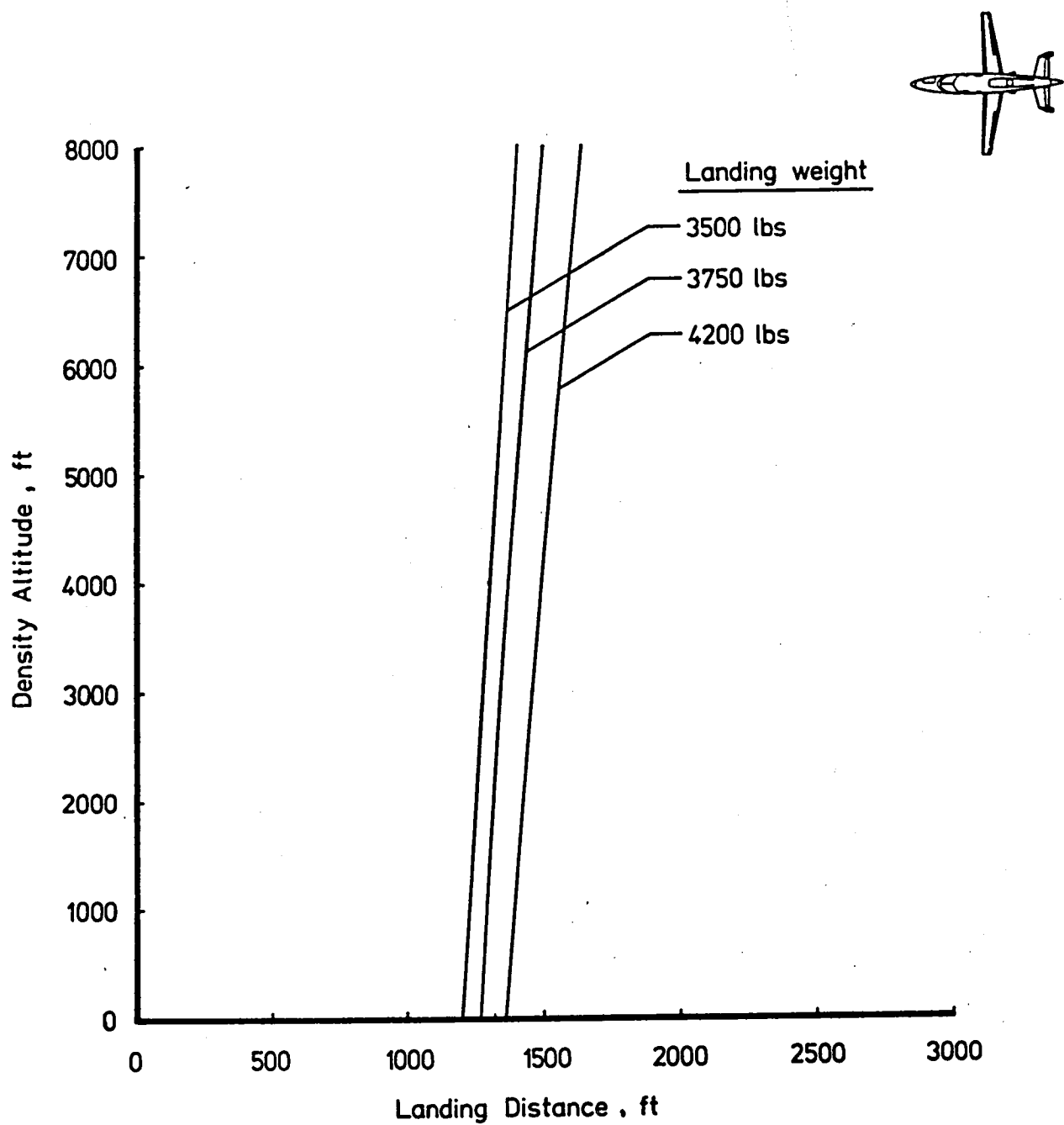
Figure 35. - GATP-2A landing distance for variations in airplane weight and altitude.

1. Report No. NASA CR-172361	2. Government Accession No.	3. Recipient's Catalog No.
4. Title and Subtitle Application of Selected Advanced Technologies to High Performance, Single-Engine, Business Airplanes		5. Report Date June 1984
		6. Performing Organization Code
7. Author(s) Christopher S. Domack and Glenn L. Martin		8. Performing Organization Report No.
9. Performing Organization Name and Address Kentron International, Incorporated Aerospace Technologies Division Hampton, Virginia 23666		10. Work Unit No.
		11. Contract or Grant No. NAS1-16000
12. Sponsoring Agency Name and Address National Aeronautics and Space Administration Washington, DC 20546		13. Type of Report and Period Covered Contractor Report
		14. Sponsoring Agency Code 505-43-43-01

15. Supplementary Notes

Langley Technical Monitor: C. E. K. Morris, Jr.

16. Abstract

A study has determined the effects of applying several advancements in the technologies for a six-place, single-turboprop, business airplane. Improvements in performance and fuel efficiency were evaluated for five new configurations derived from a conventional, aluminum-contruction baseline aircraft. Results showed the greatest performance gains for enhancements in natural laminar flow. A conceptual diesel engine provided greater fuel efficiency but reduced performance. Less significant effects were produced by the utilization of composite-materials construction or by reconfiguration from tractor to pusher-propeller installation.

17. Key Words (Suggested by Author(s)) Aircraft Configurations Turboprop Business Airplane	18. Distribution Statement Unclassified - Unlimited Star Category 05 - Aircraft Design, Testing and Performance	
19. Security Classif. (of this report) Unclassified	20. Security Classif. (of this page) Unclassified	21. No. of Pages 76
		22. Price A05

N-305